

Handbook of
**ENGINEERING
ELECTROMAGNETICS**

Edited by
Rajeev Bansal

*University of Connecticut
Storrs, Connecticut, U.S.A.*



MARCEL DEKKER

NEW YORK

6

Transmission Lines

Andreas Weisshaar

Oregon State University
Corvallis, Oregon, U.S.A.

6.1. INTRODUCTION

A *transmission line* is an electromagnetic guiding system for efficient point-to-point transmission of electric signals (information) and power. Since its earliest use in telegraphy by Samuel Morse in the 1830s, transmission lines have been employed in various types of electrical systems covering a wide range of frequencies and applications. Examples of common transmission-line applications include TV cables, antenna feed lines, telephone cables, computer network cables, printed circuit boards, and power lines. A transmission line generally consists of two or more conductors embedded in a system of dielectric media. Figure 6.1 shows several examples of commonly used types of transmission lines composed of a set of parallel conductors.

The coaxial cable (Fig. 6.1a) consists of two concentric cylindrical conductors separated by a dielectric material, which is either air or an inert gas and spacers, or a foam-filler material such as polyethylene. Owing to their self-shielding property, coaxial cables are widely used throughout the radio frequency (RF) spectrum and in the microwave frequency range. Typical applications of coaxial cables include antenna feed lines, RF signal distribution networks (e.g., cable TV), interconnections between RF electronic equipment, as well as input cables to high-frequency precision measurement equipment such as oscilloscopes, spectrum analyzers, and network analyzers.

Another commonly used transmission-line type is the two-wire line illustrated in Fig. 6.1b. Typical examples of two-wire lines include overhead power and telephone lines and the flat twin-lead line as an inexpensive antenna lead-in line. Because the two-wire line is an open transmission-line structure, it is susceptible to electromagnetic interference. To reduce electromagnetic interference, the wires may be periodically twisted (twisted pair) and/or shielded. As a result, unshielded twisted pair (UTP) cables, for example, have become one of the most commonly used types of cable for high-speed local area networks inside buildings.

Figure 6.1c–e shows several examples of the important class of planar-type transmission lines. These types of transmission lines are used, for example, in printed circuit boards to interconnect components, as interconnects in electronic packaging, and as interconnects in integrated RF and microwave circuits on ceramic or semiconducting substrates. The microstrip illustrated in Fig. 6.1c consists of a conducting strip and a

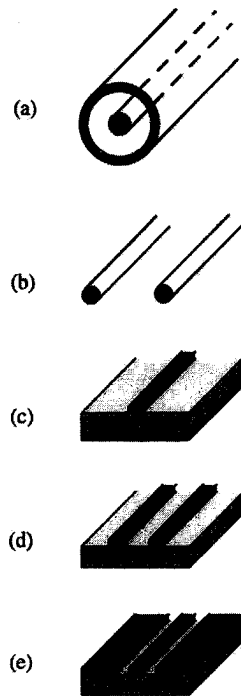


Figure 6.1 Examples of commonly used transmission lines: (a) coaxial cable, (b) two-wire line, (c) microstrip, (d) coplanar stripline, (e) coplanar waveguide.

conducting plane (ground plane) separated by a dielectric substrate. It is a widely used planar transmission line mainly because of its ease of fabrication and integration with devices and components. To connect a shunt component, however, through-holes are needed to provide access to the ground plane. On the other hand, in the coplanar stripline and coplanar waveguide (CPW) transmission lines (Fig. 6.1d and e) the conducting signal and ground strips are on the same side of the substrate. The single-sided conductor configuration eliminates the need for through-holes and is preferable for making connections to surface-mounted components.

In addition to their primary function as guiding system for signal and power transmission, another important application of transmission lines is to realize capacitive and inductive circuit elements, in particular at microwave frequencies ranging from a few gigahertz to tens of gigahertz. At these frequencies, lumped reactive elements become exceedingly small and difficult to realize and fabricate. On the other hand, transmission-line sections of appropriate lengths on the order of a quarter wavelength can be easily realized and integrated in planar transmission-line technology. Furthermore, transmission-line circuits are used in various configurations for impedance matching. The concept of functional transmission-line elements is further extended to realize a range of microwave passive components in planar transmission-line technology such as filters, couplers and power dividers [1].

This chapter on transmission lines provides a summary of the fundamental transmission-line theory and gives representative examples of important engineering applications. The following sections summarize the fundamental mathematical transmission-line equations and associated concepts, review the basic characteristics of transmission lines, present the transient response due to a step voltage or voltage pulse

as well as the sinusoidal steady-state response of transmission lines, and give practical application examples and solution techniques. The chapter concludes with a brief summary of more advanced transmission-line concepts and gives a brief discussion of current technological developments and future directions.

6.2. BASIC TRANSMISSION-LINE CHARACTERISTICS

A transmission line is inherently a distributed system that supports propagating electromagnetic waves for signal transmission. One of the main characteristics of a transmission line is the delayed-time response due to the finite wave velocity.

The transmission characteristics of a transmission line can be rigorously determined by solving Maxwell's equations for the corresponding electromagnetic problem. For an "ideal" transmission line consisting of two parallel perfect conductors embedded in a homogeneous dielectric medium, the fundamental transmission mode is a transverse electromagnetic (TEM) wave, which is similar to a plane electromagnetic wave described in the previous chapter [2]. The electromagnetic field formulation for TEM waves on a transmission line can be converted to corresponding voltage and current circuit quantities by integrating the electric field between the conductors and the magnetic field around a conductor in a given plane transverse to the direction of wave propagation [3,4].

Alternatively, the transmission-line characteristics may be obtained by considering the transmission line directly as a distributed-parameter circuit in an extension of the traditional circuit theory [5]. The distributed circuit parameters, however, need to be determined from electromagnetic field theory. The distributed-circuit approach is followed in this chapter.

6.2.1. Transmission-line Parameters

A transmission line may be described in terms of the following distributed-circuit parameters, also called *line parameters*: the inductance parameter L (in H/m), which represents the series (loop) inductance per unit length of line, and the capacitance parameter C (in F/m), which is the shunt capacitance per unit length between the two conductors. To represent line losses, the resistance parameter R (in Ω/m) is defined for the series resistance per unit length due to the finite conductivity of both conductors, while the conductance parameter G (in S/m) gives the shunt conductance per unit length of line due to dielectric loss in the material surrounding the conductors.

The R , L , G , C transmission-line parameters can be derived in terms of the electric and magnetic field quantities by relating the corresponding stored energy and dissipated power. The resulting relationships are [1,2]

$$L = \frac{\mu}{|I|^2} \int_S \mathbf{H} \cdot \mathbf{H}^* ds \quad (6.1)$$

$$C = \frac{\epsilon'}{|V|^2} \int_S \mathbf{E} \cdot \mathbf{E}^* ds \quad (6.2)$$

$$R = \frac{R_s}{|I|^2} \int_{C_1+C_2} \mathbf{H} \cdot \mathbf{H}^* dl \quad (6.3)$$

$$G = \frac{\omega \epsilon' \tan \delta}{|V|^2} \int_S \mathbf{E} \cdot \mathbf{E}^* ds \quad (6.4)$$

where \mathbf{E} and \mathbf{H} are the electric and magnetic field vectors in phasor form, "*" denotes complex conjugate operation, R_s is the surface resistance of the conductors,[†] ϵ' is the permittivity and $\tan \delta$ is the loss tangent of the dielectric material surrounding the conductors, and the line integration in Eq. (6.3) is along the contours enclosing the two conductor surfaces.

In general, the line parameters of a lossy transmission line are frequency dependent owing to the *skin effect* in the conductors and loss tangent of the dielectric medium.[‡] In the following, a lossless transmission line having constant L and C and zero R and G parameters is considered. This model represents a good first-order approximation for many practical transmission-line problems. The characteristics of lossy transmission lines are discussed in Sec. 6.4.

6.2.2. Transmission-line Equations for Lossless Lines

The fundamental equations that govern wave propagation on a lossless transmission line can be derived from an equivalent circuit representation for a short section of transmission line of length Δz illustrated in Fig. 6.2. A mathematically more rigorous derivation of the transmission-line equations is given in Ref. 5.

By considering the voltage drop across the series inductance $L\Delta z$ and current through the shunt capacitance $C\Delta z$, and taking $\Delta z \rightarrow 0$, the following fundamental transmission-line equations (also known as *telegrapher's equations*) are obtained.

$$\frac{\partial v(z, t)}{\partial z} = -L \frac{\partial i(z, t)}{\partial t} \quad (6.5)$$

$$\frac{\partial i(z, t)}{\partial z} = -C \frac{\partial v(z, t)}{\partial t} \quad (6.6)$$

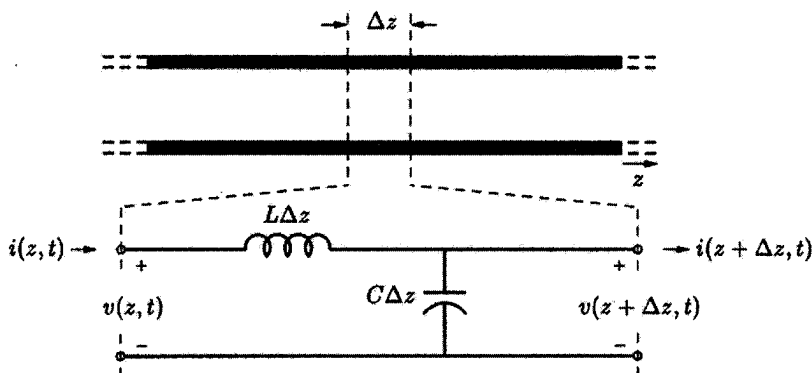


Figure 6.2 Schematic representation of a two-conductor transmission line and associated equivalent circuit model for a short section of lossless line.

[†]For a good conductor the surface resistance is $R_s = 1/\sigma\delta_s$, where the skin depth $\delta_s = 1/\sqrt{\pi f \mu \sigma}$ is assumed to be small compared to the cross-sectional dimensions of the conductor.

[‡]The skin effect describes the nonuniform current distribution inside the conductor caused by the time-varying magnetic flux within the conductor. As a result the resistance per unit length increases while the inductance per unit length decreases with increasing frequency. The loss tangent of the dielectric medium $\tan \delta = \epsilon''/\epsilon'$ typically results in an increase in shunt conductance with frequency, while the change in capacitance is negligible in most practical cases.

The transmission-line equations, Eqs. (6.5) and (6.6), can be combined to obtain a one-dimensional wave equation for voltage

$$\frac{\partial^2 v(z, t)}{\partial z^2} = LC \frac{\partial^2 v(z, t)}{\partial t^2} \quad (6.7)$$

and likewise for current.

6.2.3. General Traveling-wave Solutions for Lossless Lines

The wave equation in Eq. (6.7) has the general solution

$$v(z, t) = v^+ \left(t - \frac{z}{v_p} \right) + v^- \left(t + \frac{z}{v_p} \right) \quad (6.8)$$

where $v^+(t - z/v_p)$ corresponds to a wave traveling in the positive z direction, and $v^-(t + z/v_p)$ to a wave traveling in the negative z direction with constant velocity of propagation

$$v_p = \frac{1}{\sqrt{LC}} \quad (6.9)$$

Figure 6.3 illustrates the progression of a single traveling wave as function of position along the line and as function of time.

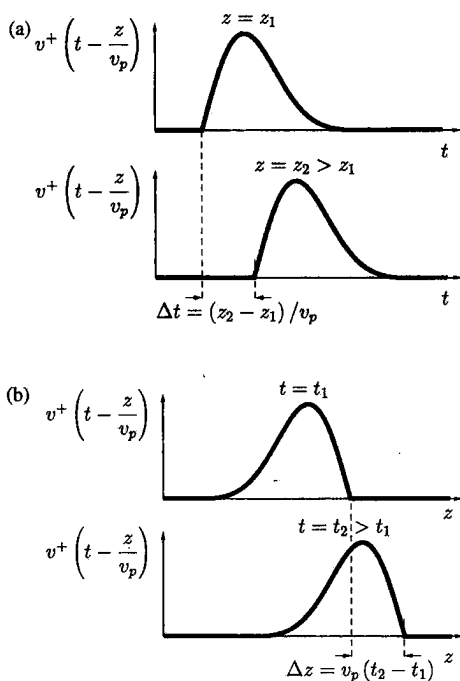


Figure 6.3 Illustration of the space and time variation for a general voltage wave $v^+(t - z/v_p)$: (a) variation in time and (b) variation in space.

A corresponding solution for sinusoidal traveling waves is

$$\begin{aligned} v(z, t) &= v_0^+ \cos \left[\omega \left(t - \frac{z}{v_p} \right) + \phi^+ \right] + v_0^- \cos \left[\omega \left(t + \frac{z}{v_p} \right) + \phi^- \right] \\ &= v_0^+ \cos (\omega t - \beta z + \phi^+) + v_0^- \cos (\omega t + \beta z + \phi^-) \end{aligned} \quad (6.10)$$

where

$$\beta = \frac{\omega}{v_p} = \frac{2\pi}{\lambda} \quad (6.11)$$

is the phase constant and $\lambda = v_p/f$ is the wavelength on the line. Since the spatial phase change βz depends on both the physical distance and the wavelength on the line, it is commonly expressed as *electrical distance* (or *electrical length*) θ with

$$\theta = \beta z = 2\pi \frac{z}{\lambda} \quad (6.12)$$

The corresponding wave solutions for current associated with voltage $v(z, t)$ in Eq. (6.8) are found with Eq. (6.5) or (6.6) as

$$i(z, t) = \frac{v^+(t - z/v_p)}{Z_0} - \frac{v^-(t + z/v_p)}{Z_0} \quad (6.13)$$

The parameter Z_0 is defined as the *characteristic impedance* of the transmission line and is given in terms of the line parameters by

$$Z_0 = \sqrt{\frac{L}{C}} \quad (6.14)$$

The characteristic impedance Z_0 specifies the ratio of voltage to current of a single traveling wave and, in general, is a function of both the conductor configuration (dimensions) and the electric and magnetic properties of the material surrounding the conductors. The negative sign in Eq. (6.13) for a wave traveling in the negative z direction accounts for the definition of positive current in the positive z direction.

As an example, consider the coaxial cable shown in Fig. 6.1a with inner conductor of diameter d , outer conductor of diameter D , and dielectric medium of dielectric constant ϵ_r . The associated distributed inductance and capacitance parameters are

$$L = \frac{\mu_0}{2\pi} \ln \frac{D}{d} \quad (6.15)$$

$$C = \frac{2\pi\epsilon_0\epsilon_r}{\ln(D/d)} \quad (6.16)$$

where $\mu_0 = 4\pi \times 10^{-7}$ H/m is the free-space permeability and $\epsilon_0 \approx 8.854 \times 10^{-12}$ F/m is the free-space permittivity. The characteristic impedance of the coaxial line is

$$Z_0 = \sqrt{\frac{L}{C}} = \frac{1}{2\pi} \sqrt{\frac{\mu_0}{\epsilon_0\epsilon_r}} \ln \frac{D}{d} = \frac{60}{\sqrt{\epsilon_r}} \ln \frac{D}{d} \quad (\Omega) \quad (6.17)$$

and the velocity of propagation is

$$v_p = \frac{1}{LC} = \frac{1}{\sqrt{\mu_0 \epsilon_0 \epsilon_r}} = \frac{c}{\sqrt{\epsilon_r}} \quad (6.18)$$

where $c \approx 30$ cm/ns is the velocity of propagation in free space.

In general, the velocity of propagation of a TEM wave on a lossless transmission line embedded in a homogeneous dielectric medium is independent of the geometry of the line and depends only on the material properties of the dielectric medium. The velocity of propagation is reduced from the free-space velocity c by the factor $1/\sqrt{\epsilon_r}$, which is also called the *velocity factor* and is typically given in percent.

For transmission lines with inhomogeneous or mixed dielectrics, such as the microstrip shown in Fig. 6.1c, the velocity of propagation depends on both the cross-sectional geometry of the line and the dielectric constants of the dielectric media. In this case, the electromagnetic wave propagating on the line is not strictly TEM, but for many practical applications can be approximated as a quasi-TEM wave. To extend Eq. (6.18) to transmission lines with mixed dielectrics, the inhomogeneous dielectric is replaced with a homogeneous dielectric of *effective dielectric constant* ϵ_{eff} giving the same capacitance per unit length as the actual structure. The effective dielectric constant is obtained as the ratio of the actual distributed capacitance C of the line to the capacitance of the same structure but with all dielectrics replaced with air:

$$\epsilon_{\text{eff}} = \frac{C}{C_{\text{air}}} \quad (6.19)$$

The velocity of propagation of the quasi-TEM wave can be expressed with Eq. (6.19) as


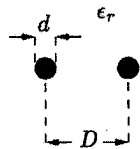
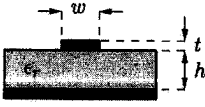
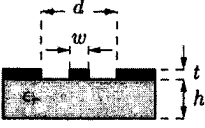
$$v_p = \frac{1}{\sqrt{\mu_0 \epsilon_0 \epsilon_{\text{eff}}}} = \frac{c}{\sqrt{\epsilon_{\text{eff}}}} \quad (6.20)$$

In general, the effective dielectric constant needs to be computed numerically; however, approximate closed-form expressions are available for many common transmission-line structures. As an example, a simple approximate closed-form expression for the effective dielectric constant of a microstrip of width w , substrate height h , and dielectric constant ϵ_r is given by [6]

$$\epsilon_{\text{eff}} = \frac{\epsilon_r + 1}{2} + \frac{\epsilon_r - 1}{2} \frac{1}{\sqrt{1 + 10h/w}} \quad (6.21)$$

Various closed-form approximations of the transmission-line parameters for many common planar transmission lines have been developed and can be found in the literature including Refs. 6 and 7. Table 6.1 gives the transmission-line parameters in exact or approximate closed form for several common types of transmission lines (assuming no losses).

Table 6.1 Transmission-line Parameters for Several Common Types of Transmission Lines

Transmission line	Parameters
 <p>Coaxial line</p>	$L = \frac{\mu_0}{2\pi} \ln(D/d)$ $C = \frac{2\pi\epsilon_0\epsilon_r}{\ln(D/d)}$ $Z_0 = \frac{1}{2\pi} \sqrt{\frac{\mu_0}{\epsilon_0\epsilon_r}} \ln(D/d)$ $\epsilon_{\text{eff}} = \epsilon_r$
 <p>Two-wire line</p>	$L = \frac{\mu_0}{\pi} \cosh^{-1}(D/d)$ $C = \frac{\pi\epsilon_0\epsilon_r}{\cosh^{-1}(D/d)}$ $Z_0 = \frac{1}{\pi} \sqrt{\frac{\mu_0}{\epsilon_0\epsilon_r}} \cosh^{-1}(D/d)$ $\epsilon_{\text{eff}} = \epsilon_r$
 <p>Microstrip</p>	$\epsilon_{\text{eff}} = \frac{\epsilon_r + 1}{2} + \frac{\epsilon_r - 1}{2} \frac{1}{\sqrt{1 + 10h/w}}$ $Z_0 = \begin{cases} \frac{60}{\sqrt{\epsilon_{\text{eff}}}} \ln\left(\frac{8h}{w} + \frac{w}{4h}\right) & \text{for } w/h \leq 1 \\ \frac{120\pi}{F\sqrt{\epsilon_{\text{eff}}}} & \text{for } w/h \geq 1 \end{cases}$ $F = w/h + 2.42 - 0.44h/w + (1 - h/w)^6$ $t \rightarrow 0 \quad [6]$
 <p>Coplanar waveguide</p>	$\epsilon_{\text{eff}} = 1 + \frac{(\epsilon_r - 1)K(k_1)K(k')}{2K(k_1)K(k)}$ $k_1 = \sqrt{1 - k^2} = \frac{\sinh[\pi w/(4h)]}{\sinh[\pi d/(4h)]}$ $k' = \sqrt{1 - k^2} = \sqrt{1 - (w/d)^2}$ $Z_0 = \frac{30}{\sqrt{\epsilon_{\text{eff}}}} \frac{K(k')}{K(k)}$ $t \rightarrow 0 \quad [6]$ <p>($K(k)$ is the elliptical integral of the first kind)</p>

6.3. TRANSIENT RESPONSE OF LOSSLESS TRANSMISSION LINES

A practical transmission line is of finite length and is necessarily terminated. Consider a transmission-line circuit consisting of a section of lossless transmission line that is connected to a source and terminated in a load, as illustrated in Fig. 6.4. The response of the transmission-line circuit depends on the transmission-line characteristics as well as the characteristics of the source and terminating load. The ideal transmission line of finite

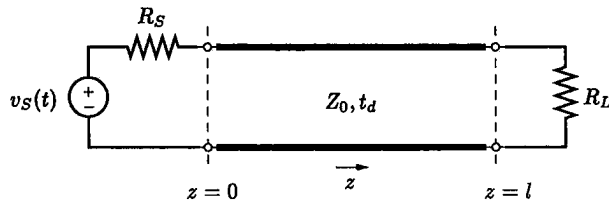


Figure 6.4 Lossless transmission line with resistive Thévenin equivalent source and resistive termination.

length is completely specified by the distributed L and C parameters and line length l , or, equivalently, by its characteristic impedance $Z_0 = \sqrt{L/C}$ and delay time

$$t_d = \frac{l}{v_p} = l\sqrt{LC} \quad (6.22)$$

of the line.* The termination imposes voltage and current boundary conditions at the end of the line, which may give rise to wave reflections.

6.3.1. Reflection Coefficient

When a traveling wave reaches the end of the transmission line, a reflected wave is generated unless the termination presents a load condition that is equal to the characteristic impedance of the line. The ratio of reflected voltage to incident voltage at the termination is defined as *voltage reflection coefficient* ρ , which for linear resistive terminations can be directly expressed in terms of the terminating resistance and the characteristic impedance of the line. The corresponding current reflection coefficient is given by $-\rho$. For the transmission-line circuit shown in Fig. 6.4 with resistive terminations, the voltage reflection coefficient at the termination with load resistance R_L is

$$\rho_L = \frac{R_L - Z_0}{R_L + Z_0} \quad (6.23)$$

Similarly, the voltage reflection coefficient at the source end with source resistance R_S is

$$\rho_S = \frac{R_S - Z_0}{R_S + Z_0} \quad (6.24)$$

The inverse relationship between reflection coefficient ρ_L and load resistance R_L follows directly from Eq. (6.23) and is

$$R_L = \frac{1 + \rho_L}{1 - \rho_L} Z_0 \quad (6.25)$$

*The specification in terms of characteristic impedance and delay time is used, for example, in the standard SPICE model for an ideal transmission line [8].

It is seen from Eq. (6.23) or (6.24) that the reflection coefficient is positive for a termination resistance greater than the characteristic impedance, and it is negative for a termination resistance less than the characteristic impedance of the line. A termination resistance equal to the characteristic impedance produces no reflection ($\rho = 0$) and is called *matched termination*. For the special case of an open-circuit termination the voltage reflection coefficient is $\rho_{oc} = +1$, while for a short-circuit termination the voltage reflection coefficient is $\rho_{sc} = -1$.

6.3.2. Step Response

To illustrate the wave reflection process, the step-voltage response of an ideal transmission line connected to a Thévenin equivalent source and terminated in a resistive load, as shown in Fig. 6.4, is considered. The transient response for a step-voltage change with finite rise time can be obtained in a similar manner. The step-voltage response of a *lossy* transmission line with constant or frequency-dependent line parameters is more complex and can be determined using the Laplace transformation [5].

The source voltage $v_S(t)$ in the circuit in Fig. 6.4 is assumed to be a step-voltage given by

$$v_S(t) = V_0 U(t) \quad (6.26)$$

where

$$U(t) = \begin{cases} 1 & \text{for } t \geq 0 \\ 0 & \text{for } t < 0 \end{cases} \quad (6.27)$$

The transient response due to a rectangular pulse $v_{\text{pulse}}(t)$ of duration T can be obtained as the superposition of two step responses given as $v_{\text{pulse}}(t) = V_0 U(t) - V_0 U(t - T)$.

The step-voltage change launches a forward traveling wave at the input of the line at time $t = 0$. Assuming no initial charge or current on the line, this first wave component presents a resistive load to the generator that is equal to the characteristic impedance of the line. The voltage of the first traveling wave component is

$$v_1^+(z, t) = V_0 \frac{Z_0}{R_S + Z_0} U\left(t - \frac{z}{v_p}\right) = V_1^+ U\left(t - \frac{z}{v_p}\right) \quad (6.28)$$

where v_p is the velocity of propagation on the line. For a nonzero reflection coefficient ρ_L at the termination, a reflected wave is generated when the first traveling wave arrives at the termination at time $t = t_d = l/v_p$. If the reflection coefficients at both the source and the termination are nonzero, an infinite succession of reflected waves results. The total voltage

response on the line is the superposition of all traveling-wave components and is given by

$$\begin{aligned}
 v(z, t) = & \frac{Z_0}{R_S + Z_0} V_0 \left[U\left(t - \frac{z}{v_p}\right) + \rho_L U\left(t - 2t_d + \frac{z}{v_p}\right) \right. \\
 & + \rho_S \rho_L U\left(t - 2t_d - \frac{z}{v_p}\right) + \rho_S \rho_L^2 U\left(t - 4t_d + \frac{z}{v_p}\right) \\
 & + \rho_S^2 \rho_L^2 U\left(t - 4t_d - \frac{z}{v_p}\right) + \rho_S^2 \rho_L^3 U\left(t - 6t_d + \frac{z}{v_p}\right) \\
 & \left. + \dots \right] \quad (6.29)
 \end{aligned}$$

Similarly, the total current on the line is given by

$$\begin{aligned}
 i(z, t) = & \frac{V_0}{R_S + Z_0} \left[U\left(t - \frac{z}{v_p}\right) - \rho_L U\left(t - 2t_d + \frac{z}{v_p}\right) \right. \\
 & + \rho_S \rho_L U\left(t - 2t_d - \frac{z}{v_p}\right) - \rho_S \rho_L^2 U\left(t - 4t_d + \frac{z}{v_p}\right) \\
 & + \rho_S^2 \rho_L^2 U\left(t - 4t_d - \frac{z}{v_p}\right) - \rho_S^2 \rho_L^3 U\left(t - 6t_d + \frac{z}{v_p}\right) \\
 & \left. + \dots \right] \quad (6.30)
 \end{aligned}$$

The reflected wave components on the lossless transmission line are successively delayed copies of the first traveling-wave component with amplitudes appropriately adjusted by the reflection coefficients. Equations (6.29) and (6.30) show that at any given time and location on the line only a finite number of wave components have been generated. For example, for $t = 3t_d$ three wave components exist at the input of the line (at $z = 0$) and four wave components exist at the load (at $z = l$).

Unless both reflection coefficients have unity magnitudes, the amplitudes of the successive wave components become progressively smaller in magnitude and the infinite summations in Eqs. (6.29) and (6.30) converge to the dc values for $t \rightarrow \infty$. The steady-state (dc) voltage V_∞ is obtained by summing the amplitudes of all traveling-wave components for $t \rightarrow \infty$.

$$\begin{aligned}
 V_\infty = v(z, t \rightarrow \infty) &= \frac{Z_0}{R_S + Z_0} V_0 \{1 + \rho_L + \rho_S \rho_L + \rho_S \rho_L^2 + \rho_S^2 \rho_L^2 + \dots\} \\
 &= \frac{Z_0}{R_S + Z_0} V_0 \frac{1 + \rho_L}{1 - \rho_S \rho_L} \quad (6.31)
 \end{aligned}$$

The steady-state voltage can also be directly obtained as the dc voltage drop across the load after removing the lossless line, that is

$$V_\infty = \frac{R_L}{R_S + R_L} V_0 \quad (6.32)$$

The steady-state current is

$$I_{\infty} = \frac{V_0}{R_S + R_L} \tag{6.33}$$

6.3.3. Lattice Diagram

The *lattice diagram* (also called *bounce* or *reflection diagram*) provides a convenient graphical means for keeping track of the multiple wave reflections on the line. The general lattice diagram is illustrated in Fig. 6.5. Each wave component is represented by a sloped line segment that shows the time elapsed after the initial voltage change at the source as a function of distance z on the line. For bookkeeping purposes, the value of the voltage amplitude of each wave component is commonly written above the corresponding line segment and the value of the accompanying current is added below. Starting with voltage $V_1^+ = V_0 Z_0 / (R_S + Z_0)$ of the first wave component, the voltage amplitude of each successive wave is obtained from the voltage of the preceding wave by multiplication with the appropriate reflection coefficient ρ_L or ρ_S in accordance with Eq. (6.29). Successive current values are obtained by multiplication with $-\rho_L$ or $-\rho_S$, as shown in Eq. (6.30).

The lattice diagram may be conveniently used to determine the voltage and current distributions along the transmission line at any given time or to find the time response at any given position. The variation of voltage and current as a function of time at a given position $z = z_1$ is found from the intersection of the vertical line through z_1 and the sloped line segments representing the wave components. Figure 6.5 shows the first five wave intersection times at position z_1 marked as $t_1, t_2, t_3, t_4,$ and t_5 , respectively. At each

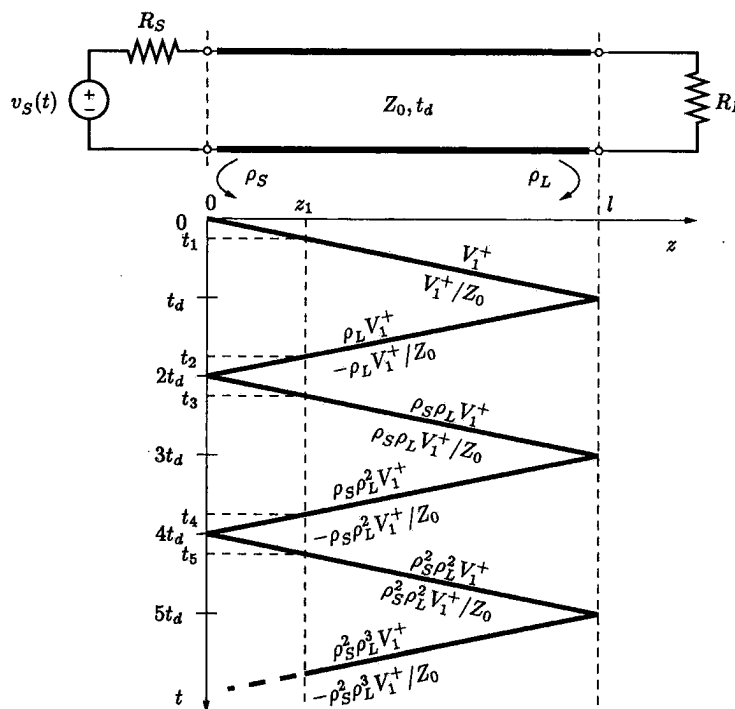


Figure 6.5 Lattice diagram for a lossless transmission line with unmatched terminations.

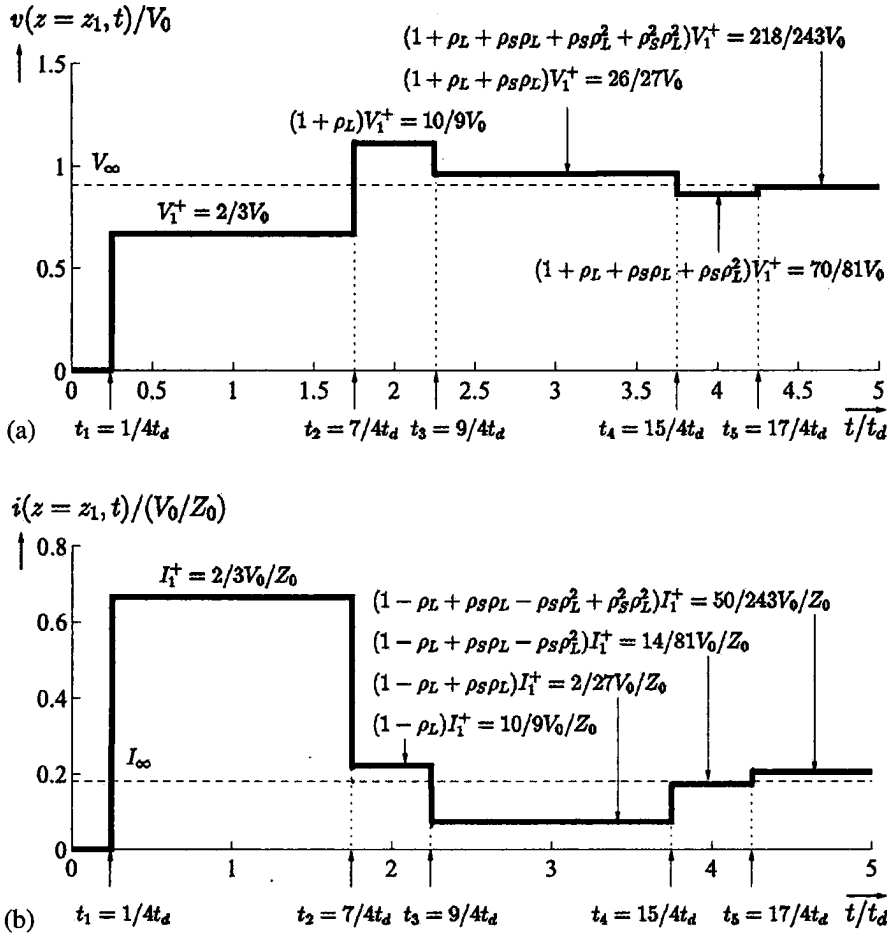


Figure 6.6 Step response of a lossless transmission line at $z = z_1 = l/4$ for $R_S = Z_0/2$ and $R_L = 5Z_0$; (a) voltage response, (b) current response.

intersection time, the total voltage and current change by the amplitudes specified for the intersecting wave component. The corresponding transient response for voltage and current with $R_S = Z_0/2$ and $R_L = 5Z_0$ corresponding to reflection coefficients $\rho_S = -1/3$ and $\rho_L = 2/3$, respectively, is shown in Fig. 6.6. The transient response converges to the steady-state $V_\infty = 10/11 V_0$ and $I_\infty = 2/11(V_0/Z_0)$, as indicated in Fig. 6.6.

6.3.4. Applications

In many practical applications, one or both ends of a transmission line are matched to avoid multiple reflections. If the source and/or the receiver do not provide a match, multiple reflections can be avoided by adding an appropriate resistor at the input of the line (source termination) or at the end of the line (end termination) [9,10]. Multiple reflections on the line may lead to signal distortion including a slow voltage buildup or signal overshoot and ringing.

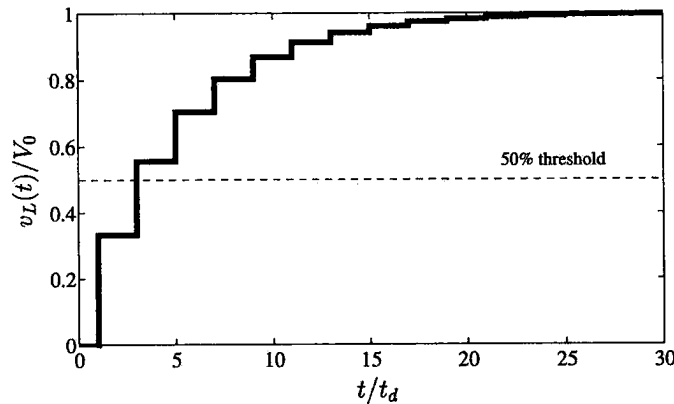


Figure 6.7 Step-voltage response at the termination of an open-circuited lossless transmission line with $R_S = 5Z_0$ ($\rho_S = 2/3$).

Over- and Under-driven Transmission Lines

In high-speed digital systems, the input of a receiver circuit typically presents a load to a transmission line that is approximately an open circuit (unterminated). The step-voltage response of an unterminated transmission line may exhibit a considerably different behavior depending on the source resistance.

If the source resistance is larger than the characteristic impedance of the line, the voltage across the load will build up monotonically to its final value since both reflection coefficients are positive. This condition is referred to as an *underdriven* transmission line. The buildup time to reach a sufficiently converged voltage may correspond to many round-trip times if the reflection coefficient at the source is close to $+1$ (and $\rho_L = \rho_{oc} = +1$), as illustrated in Fig. 6.7. As a result, the effective signal delay may be several times longer than the delay time of the line.

If the source resistance is smaller than the characteristic impedance of the line, the initial voltage at the unterminated end will exceed the final value (overshoot). Since the source reflection coefficient is negative and the load reflection coefficient is positive, the voltage response will exhibit ringing as the voltage converges to its final value. This condition is referred to as an *overdriven* transmission line. It may take many round-trip times to reach a sufficiently converged voltage (long settling time) if the reflection coefficient at the source is close to -1 (and $\rho_L = \rho_{oc} = +1$), as illustrated in Fig. 6.8. An overdriven line can produce excessive noise and cause intersymbol interference.

Transmission-line Junctions

Wave reflections occur also at the junction of two tandem-connected transmission lines having different characteristic impedances. This situation, illustrated in Fig. 6.9a, is often encountered in practice. For an incident wave on line 1 with characteristic impedance $Z_{0,1}$, the second line with characteristic impedance $Z_{0,2}$ presents a load resistance to line 1 that is equal to $Z_{0,2}$. At the junction, a reflected wave is generated on line 1 with voltage reflection coefficient ρ_{11} given by

$$\rho_{11} = \frac{Z_{0,2} - Z_{0,1}}{Z_{0,2} + Z_{0,1}} \quad (6.34)$$

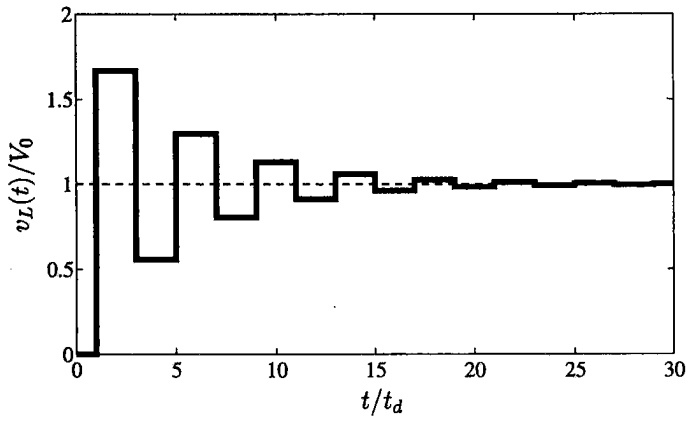


Figure 6.8 Step-voltage response at the termination of an open-circuited lossless transmission line with $R_S = Z_0/5$ ($\rho_S = -2/3$).

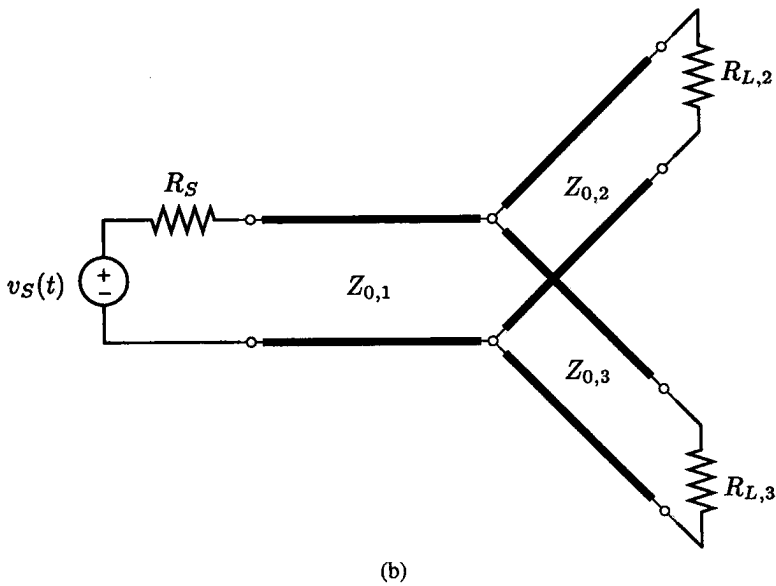
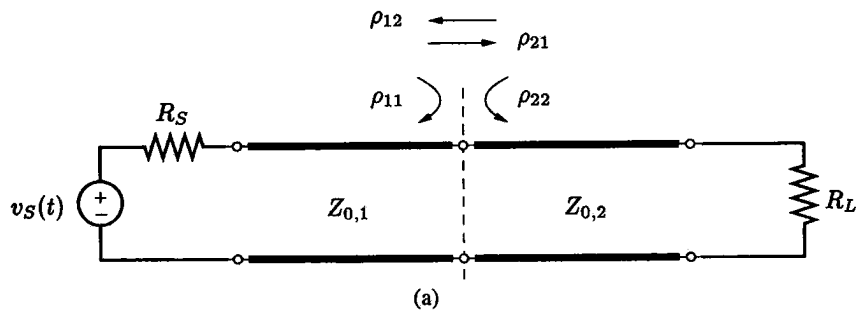


Figure 6.9 Junction between transmission lines: (a) two tandem-connected lines and (b) three parallel-connected lines.

In addition, a wave is launched on the second line departing from the junction. The voltage amplitude of the transmitted wave is the sum of the voltage amplitudes of the incident and reflected waves on line 1. The ratio of the voltage amplitudes of the transmitted wave on line 2 to the incident wave on line 1 is defined as the *voltage transmission coefficient* ρ_{21} and is given by

$$\rho_{21} = 1 + \rho_{11} = \frac{2Z_{0,2}}{Z_{0,1} + Z_{0,2}} \quad (6.35)$$

Similarly, for an incident wave from line 2, the reflection coefficient ρ_{22} at the junction is

$$\rho_{22} = \frac{Z_{0,1} - Z_{0,2}}{Z_{0,1} + Z_{0,2}} = -\rho_{11} \quad (6.36)$$

The voltage transmission coefficient ρ_{12} for a wave incident from line 2 and transmitted into line 1 is

$$\rho_{12} = 1 + \rho_{22} = \frac{2Z_{0,1}}{Z_{0,1} + Z_{0,2}} \quad (6.37)$$

If in addition lumped elements are connected at the junction or the transmission lines are connected through a resistive network, the reflection and transmission coefficients will change, and in general, $\rho_{ij} \leq 1 + \rho_{ij}$ [5].

For a parallel connection of multiple lines at a common junction, as illustrated in Fig. 6.9b, the effective load resistance is obtained as the parallel combination of the characteristic impedances of all lines except for the line carrying the incident wave. The reflection and transmission coefficients are then determined as for tandem connected lines [5].

The wave reflection and transmission process for tandem and multiple parallel-connected lines can be represented graphically with a lattice diagram for each line. The complexity, however, is significantly increased over the single line case, in particular if multiple reflections exist.

Reactive Terminations

In various transmission-line applications, the load is not purely resistive but has a reactive component. Examples of reactive loads include the capacitive input of a CMOS gate, pad capacitance, bond-wire inductance, as well as the reactance of vias, package pins, and connectors [9,10]. When a transmission line is terminated in a reactive element, the reflected waveform will not have the same shape as the incident wave, i.e., the reflection coefficient will not be a constant but be varying with time. For example, consider the step response of a transmission line that is terminated in an uncharged capacitor C_L . When the incident wave reaches the termination, the initial response is that of a short circuit, and the response after the capacitor is fully charged is an open circuit. Assuming the source end is matched to avoid multiple reflections, the incident step-voltage wave is $v_1^+(t) = V_0/2U(t - z/v_p)$. The voltage across the capacitor changes exponentially from the initial voltage $v_{\text{cap}} = 0$ (short circuit) at time $t = t_d$ to the final voltage

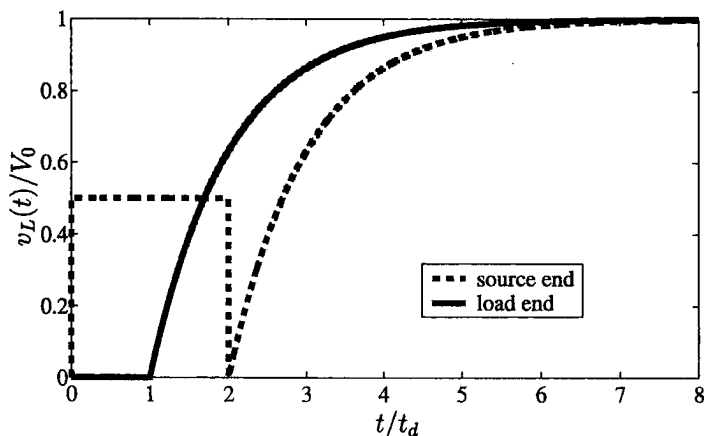


Figure 6.10 Step-voltage response of a transmission line that is matched at the source and terminated in a capacitor C_L with time constant $\tau = Z_0 C_L = t_d$.

$v_{\text{cap}}(t \rightarrow \infty) = V_0$ (open circuit) as

$$v_{\text{cap}}(t) = V_0 [1 - e^{-(t-t_d)/\tau}] U(t-t_d) \quad (6.38)$$

with time constant

$$\tau = Z_0 C_L \quad (6.39)$$

where Z_0 is the characteristic impedance of the line. Figure 6.10 shows the step-voltage response across the capacitor and at the source end of the line for $\tau = t_d$.

If the termination consists of a parallel combination of a capacitor C_L and a resistor R_L , the time constant is obtained as the product of C_L and the parallel combination of R_L and characteristic impedance Z_0 . For a purely inductive termination L_L , the initial response is an open circuit and the final response is a short circuit. The corresponding time constant is $\tau = L_L/Z_0$.

In the general case of reactive terminations with multiple reflections or with more complicated source voltages, the boundary conditions for the reactive termination are expressed in terms of a differential equation. The transient response can then be determined mathematically, for example, using the Laplace transformation [11].

Nonlinear Terminations

For a nonlinear load or source, the reflected voltage and subsequently the reflection coefficient are a function of the cumulative voltage and current at the termination including the contribution of the reflected wave to be determined. Hence, the reflection coefficient for a nonlinear termination cannot be found from only the termination characteristics and the characteristic impedance of the line. The step-voltage response for each reflection instance can be determined by matching the I - V characteristics of the termination and the cumulative voltage and current characteristics at the end of the transmission line. This solution process can be constructed using a graphical technique known as the *Bergeron method* [5,12] and can be implemented in a computer program.

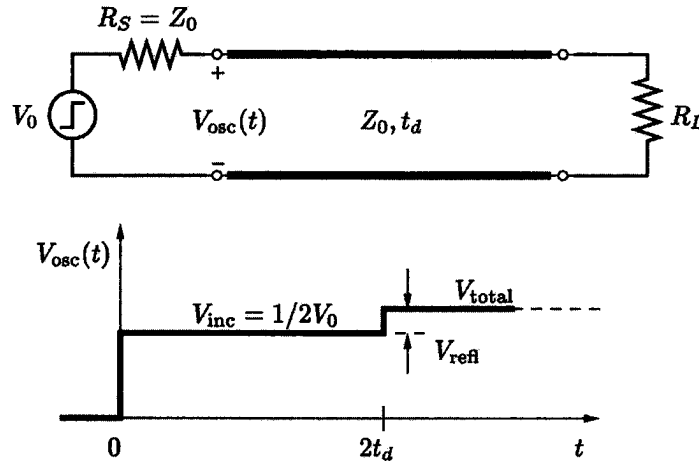


Figure 6.11 Illustration of the basic principle of time-domain reflectometry (TDR).

Time-Domain Reflectometry

Time-domain reflectometry (TDR) is a measurement technique that utilizes the information contained in the reflected waveform and observed at the source end to test, characterize, and model a transmission-line circuit. The basic TDR principle is illustrated in Fig. 6.11. A TDR instrument typically consists of a precision step-voltage generator with a known source (reference) impedance to launch a step wave on the transmission-line circuit under test and a high impedance probe and oscilloscope to sample and display the voltage waveform at the source end. The source end is generally well matched to establish a reflection-free reference. The voltage at the input changes from the initial incident voltage when a reflected wave generated at an impedance discontinuity such as a change in line impedance, a line break, an unwanted parasitic reactance, or an unmatched termination reaches the source end of the transmission line-circuit.

The time elapsed between the initial launch of the step wave and the observation of the reflected wave at the input corresponds to the round-trip delay $2t_d$ from the input to the location of the impedance mismatch and back. The round-trip delay time can be converted to find the distance from the input of the line to the location of the impedance discontinuity if the propagation velocity is known. The capability of measuring distance is used in TDR cable testers to locate faults in cables. This measurement approach is particularly useful for testing long, inaccessible lines such as underground or undersea electrical cables.

The reflected waveform observed at the input also provides information on the type of discontinuity and the amount of impedance change. Table 6.2 shows the TDR response for several common transmission-line discontinuities. As an example, the load resistance in the circuit in Fig. 6.11 is extracted from the incident and reflected or total voltage observed at the input as

$$R_L = Z_0 \frac{1 + \rho}{1 - \rho} = Z_0 \frac{V_{\text{total}}}{2V_{\text{incident}} - V_{\text{total}}} \quad (6.40)$$

where $\rho = V_{\text{reflected}}/V_{\text{incident}} = (R_L - Z_0)/(R_L + Z_0)$ and $V_{\text{total}} = V_{\text{incident}} + V_{\text{reflected}}$.

Table 6.2 TDR Responses for Typical Transmission-line Discontinuities.

TDR response	Circuit

The TDR principle can be used to profile impedance changes along a transmission line circuit such as a trace on a printed-circuit board. In general, the effects of multiple reflections arising from the impedance mismatches along the line need to be included to extract the impedance profile. If the mismatches are small, higher-order reflections can be ignored and the same extraction approach as for a single impedance discontinuity can be applied for each discontinuity. The resolution of two closely spaced discontinuities, however, is limited by the rise time of step voltage and the overall rise time of the TDR system. Further information on using time-domain reflectometry for analyzing and modeling transmission-line systems is given e.g. in Refs. 10,11,13-15.

6.4. SINUSOIDAL STEADY-STATE RESPONSE OF TRANSMISSION LINES

The steady-state response of a transmission line to a sinusoidal excitation of a given frequency serves as the fundamental solution for many practical transmission-line applications including radio and television broadcast and transmission-line circuits operating at microwave frequencies. The frequency-domain information also provides physical insight into the signal propagation on the transmission line. In particular, transmission-line losses and any frequency dependence in the R , L , G , C line parameters can be readily taken into account in the frequency-domain analysis of transmission lines. The time-domain response of a transmission-line circuit to an arbitrary time-varying excitation can then be obtained from the frequency-domain solution by applying the concepts of Fourier analysis [16].

As in standard circuit analysis, the time-harmonic voltage and current on the transmission line are conveniently expressed in phasor form using Euler's identity $e^{j\theta} = \cos \theta + j \sin \theta$. For a cosine reference, the relations between the voltage and current phasors, $V(z)$ and $I(z)$, and the time-harmonic space-time-dependent quantities, $v(z, t)$ and $i(z, t)$, are

$$v(z, t) = \text{Re}\{V(z)e^{j\omega t}\} \quad (6.41)$$

$$i(z, t) = \text{Re}\{I(z)e^{j\omega t}\} \quad (6.42)$$

The voltage and current phasors are functions of position z on the transmission line and are in general complex.

6.4.1. Characteristics of Lossy Transmission Lines

The transmission-line equations, (general telegrapher's equations) in phasor form for a general lossy transmission line can be derived directly from the equivalent circuit for a short line section of length $\Delta z \rightarrow 0$ shown in Fig. 6.12. They are

$$-\frac{dV(z)}{dz} = (R + j\omega L)I(z) \quad (6.43)$$

$$-\frac{dI(z)}{dz} = (G + j\omega C)V(z) \quad (6.44)$$

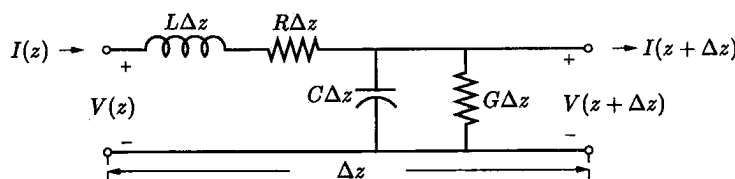


Figure 6.12 Equivalent circuit model for a short section of lossy transmission line of length Δz with R , L , G , C line parameters.

The transmission-line equations, Eqs. (6.43) and (6.44) can be combined to the complex wave equation for voltage (and likewise for current)

$$\frac{d^2 V(z)}{dz^2} = (R + j\omega L)(G + j\omega C)V(z) = \gamma^2 V(z) \quad (6.45)$$

The general solution of Eq. (6.45) is

$$V(z) = V^+(z) + V^-(z) = V_0^+ e^{-\gamma z} + V_0^- e^{+\gamma z} \quad (6.46)$$

where γ is the *propagation constant* of the transmission line and is given by

$$\gamma = \alpha + j\beta = \sqrt{(R + j\omega L)(G + j\omega C)} \quad (6.47)$$

and $V_0^+ = |V_0^+|e^{j\phi^+}$ and $V_0^- = |V_0^-|e^{j\phi^-}$ are complex constants. The real time-harmonic voltage waveforms $v(z, t)$ corresponding to phasor $V(z)$ are obtained with Eq. (6.41) as

$$\begin{aligned} v(z, t) &= v^+(z, t) + v^-(z, t) \\ &= |V_0^+|e^{-\alpha z} \cos(\omega t - \beta z + \phi^+) + |V_0^-|e^{\alpha z} \cos(\omega t + \beta z + \phi^-) \end{aligned} \quad (6.48)$$

and are illustrated in Fig. 6.13.

The real part α of the propagation constant in Eq. (6.47) is known as the *attenuation constant* measured in nepers per unit length (Np/m) and gives the rate of exponential attenuation of the voltage and current amplitudes of a traveling wave.* The imaginary part of γ is the *phase constant* $\beta = 2\pi/\lambda$ measured in radians per unit length (rad/m), as in the lossless line case. The corresponding *phase velocity* of the time-harmonic wave is given by

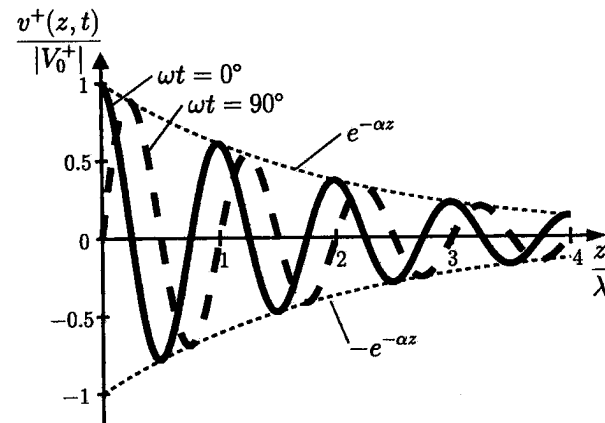
$$v_p = \frac{\omega}{\beta} \quad (6.49)$$

which depends in general on frequency. Transmission lines with frequency-dependent phase velocity are called *dispersive* lines. Dispersive transmission lines can lead to signal distortion, in particular for broadband signals.

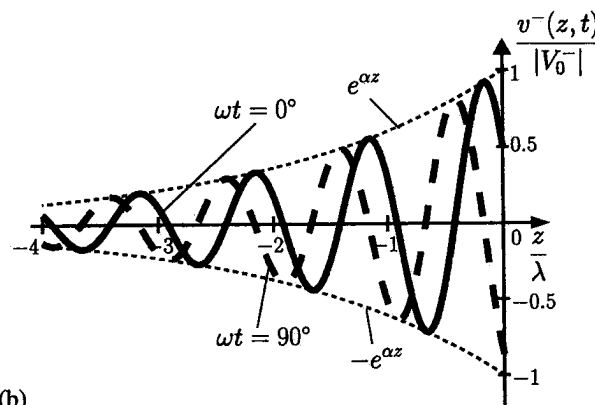
The current phasor $I(z)$ associated with voltage $V(z)$ in Eq. (6.46) is found with Eq. (6.43) as

$$I(z) = \frac{V^+}{Z_0} e^{-\gamma z} - \frac{V^-}{Z_0} e^{+\gamma z} \quad (6.50)$$

*The amplitude attenuation of a traveling wave $V^+(z) = V_0^+ e^{-\gamma z} = V_0^+ e^{-\alpha z} e^{-j\beta z}$ over a distance l can be expressed in logarithmic form as $\ln |V^+(z)/V^+(z+l)| = \alpha l$ (nepers). To convert from the attenuation measured in nepers to the logarithmic measure $20 \log_{10} |V^+(z)/V^+(z+l)|$ in dB, the attenuation in nepers is multiplied by $20 \log_{10} e \approx 8.686$ (1 Np corresponds to about 8.686 dB). For coaxial cables the attenuation constant is typically specified in units of dB/100 ft. The conversion to Np/m is 1 dB/100 ft \approx 0.0038 Np/m.



(a)



(b)

Figure 6.13 Illustration of a traveling wave on a lossy transmission line: (a) wave traveling in $+z$ direction with $\phi^+ = 0$ and $\alpha = 1/(2\lambda)$ and (b) wave traveling in $-z$ direction with $\phi^- = 60^\circ$ and $\alpha = 1/(2\lambda)$.

The quantity Z_0 is defined as the characteristic impedance of the transmission line and is given in terms of the line parameters by

$$Z_0 = \sqrt{\frac{R + j\omega L}{G + j\omega C}} \quad (6.51)$$

As seen from Eq. (6.51), the characteristic impedance is in general complex and frequency dependent.

The inverse expressions relating the R , L , G , C line parameters to the characteristic impedance and propagation constant of a transmission line are found from Eqs. (6.47) and (6.51) as

$$R + j\omega L = \gamma Z_0 \quad (6.52)$$

$$G + j\omega C = \gamma / Z_0 \quad (6.53)$$

These inverse relationships are particularly useful for extracting the line parameters from experimentally determined data for characteristic impedance and propagation constant.

Special Cases

For a lossless line with $R=0$ and $G=0$, the propagation constant is $\gamma = j\omega\sqrt{LC}$. The attenuation constant α is zero and the phase velocity is $v_p = \omega/\beta = 1/\sqrt{LC}$. The characteristic impedance of a lossless line is $Z_0 = \sqrt{L/C}$, as in Eq. (6.14).

In general, for a lossy transmission line both the attenuation constant and the phase velocity are frequency dependent, which can give rise to signal distortion.* However, in many practical applications the losses along the transmission line are small. For a low loss line with $R \ll \omega L$ and $G \ll \omega C$, useful approximate expressions can be derived for the characteristic impedance Z_0 and propagation constant γ as

$$Z_0 \approx \sqrt{\frac{L}{C}} \left[1 - j \frac{1}{2\omega} \left(\frac{R}{L} - \frac{G}{C} \right) \right] \quad (6.54)$$

and

$$\gamma \approx \frac{R}{2} \sqrt{\frac{C}{L}} + \frac{G}{2} \sqrt{\frac{L}{C}} + j\omega\sqrt{LC} \quad (6.55)$$

The low-loss conditions $R \ll \omega L$ and $G \ll \omega C$ are more easily satisfied at higher frequencies.

6.4.2. Terminated Transmission lines

If a transmission line is terminated with a load impedance that is different from the characteristic impedance of the line, the total time-harmonic voltage and current on the line will consist of two wave components traveling in opposite directions, as given by the general phasor expressions in Eqs. (6.46) and (6.50). The presence of the two wave components gives rise to standing waves on the line and affects the line's input impedance.

Impedance Transformation

Figure 6.14 shows a transmission line of finite length terminated with load impedance Z_L . In the steady-state analysis of transmission-line circuits it is expedient to measure distance on the line from the termination with known load impedance. The distance on the line from the termination is given by z' . The line voltage and current at distance z' from the

*For the special case of a line satisfying the condition $R/L = G/C$, the characteristic impedance $Z_0 = \sqrt{L/C}$, the attenuation constant $\alpha = R/\sqrt{L/C}$, and the phase velocity $v_p = 1/\sqrt{LC}$ are frequency independent. This type of line is called a *distortionless line*. Except for a constant signal attenuation, a distortionless line behaves like a lossless line.

termination can be related to voltage $V_L = V(z' = 0)$ and current $I_L = I(z' = 0)$ at the termination as

$$V(z') = V_L \cosh \gamma z' + I_L Z_0 \sinh \gamma z' \quad (6.56)$$

$$I(z') = V_L \left(\frac{1}{Z_0} \right) \sinh \gamma z' + I_L \cosh \gamma z' \quad (6.57)$$

where $V_L/I_L = Z_L$. These voltage and current transformations between the input and output of a transmission line of length z' can be conveniently expressed in $ABCD$ matrix form as*

$$\begin{bmatrix} V(z') \\ I(z') \end{bmatrix} = \begin{bmatrix} A & B \\ C & D \end{bmatrix} \begin{bmatrix} V(0) \\ I(0) \end{bmatrix} = \begin{bmatrix} \cosh(\gamma z') & Z_0 \sinh(\gamma z') \\ (1/Z_0) \sinh(\gamma z') & \cosh(\gamma z') \end{bmatrix} \begin{bmatrix} V(0) \\ I(0) \end{bmatrix} \quad (6.58)$$

The ratio $V(z')/I(z')$ defines the input impedance $Z_{in}(z')$ at distance z' looking toward the load. The input impedance for a general lossy line with characteristic impedance Z_0 and terminated with load impedance Z_L is

$$Z_{in}(z') = \frac{V(z')}{I(z')} = Z_0 \frac{Z_L + Z_0 \tanh \gamma z'}{Z_0 + Z_L \tanh \gamma z'} \quad (6.60)$$

It is seen from Eq. (6.60) that for a line terminated in its characteristic impedance ($Z_L = Z_0$), the input impedance is identical to the characteristic impedance, independent of distance z' . This property serves as an alternate definition of the characteristic impedance of a line and can be applied to experimentally determine the characteristic impedance of a given line.

The input impedance of a transmission line can be used advantageously to determine the voltage and current at the input terminals of a transmission-line circuit as well as the average power delivered by the source and ultimately the average power dissipated in the load. Figure 6.15 shows the equivalent circuit at the input (source end) for the transmission-line circuit in Fig. 6.14. The input voltage V_{in} and current I_{in} are easily

*The $ABCD$ matrix is a common representation for two-port networks and is particularly useful for cascade connections of two or more two-port networks. The overall voltage and current transformations for cascaded lines and lumped elements can be easily obtained by multiplying the corresponding $ABCD$ matrices of the individual sections [1]. For a lossless transmission line, the $ABCD$ parameters are

$$\begin{bmatrix} A & B \\ C & D \end{bmatrix}_{\text{lossless line}} = \begin{bmatrix} \cos \theta & jZ_0 \sin \theta \\ (j/Z_0) \sin \theta & \cos \theta \end{bmatrix} \quad (6.59)$$

where $\theta = \beta z'$ is the electrical length of the line segment.

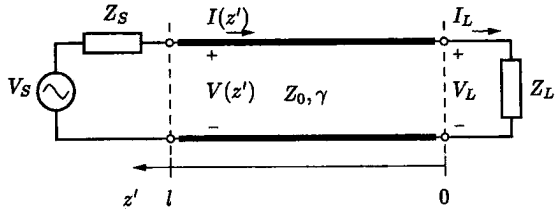


Figure 6.14 Transmission line of finite length terminated in load impedance Z_L .

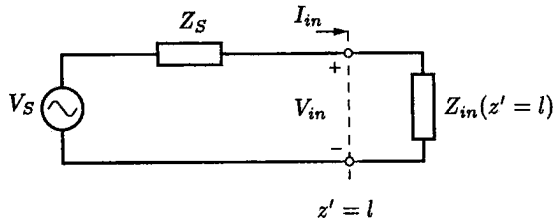


Figure 6.15 Equivalent circuit at the input of the transmission line circuit shown in Fig. 6.14.

determined from the voltage divider circuit. The average power delivered by the source to the input terminals of the transmission line is

$$P_{\text{ave, in}} = \frac{1}{2} \text{Re}\{V_{\text{in}} I_{\text{in}}^*\} \tag{6.61}$$

The average power dissipated in the load impedance $Z_L = R_L + jX_L$ is

$$P_{\text{ave, L}} = \frac{1}{2} \text{Re}\{V_L I_L^*\} = \frac{1}{2} |I_L|^2 R_L = \frac{1}{2} \left| \frac{V_L}{Z_L} \right|^2 R_L \tag{6.62}$$

where V_L and I_L can be determined from the inverse of the $ABCD$ matrix transformation Eq. (6.58).^{*} In general, $P_{\text{ave, L}} < P_{\text{ave, in}}$ for a lossy line and $P_{\text{ave, L}} = P_{\text{ave, in}}$ for a lossless line.

Example. Consider a 10 m long low-loss coaxial cable of nominal characteristic impedance $Z_0 = 75 \Omega$, attenuation constant $\alpha = 2.2$ dB per 100 ft at 100 MHz, and velocity factor of 78%. The line is terminated in $Z_L = 100 \Omega$, and the circuit is operated at $f = 100$ MHz. The $ABCD$ parameters for the transmission line are $A = D = -0.1477 + j0.0823$, $B = (-0.9181 + j74.4399) \Omega$, and $C = (-0.0002 + j0.0132) \Omega^{-1}$. The input impedance of the line is found as $Z_{\text{in}} = (59.3 + j4.24) \Omega$. For a source voltage $|V_S| = 10$ V and source impedance $Z_S = 75 \Omega$, the average power delivered to the input of the line is $P_{\text{ave, in}} = 164.2$ mW and the average power dissipated in the load impedance is $P_{\text{ave, L}} = 138.3$ mW. The difference of 25.9 mW ($\approx 16\%$ of the input power) is dissipated in the transmission line.

^{*}The inverse of Eq. (6.58) expressing the voltage and current at the load in terms of the input voltage and current is

$$\begin{bmatrix} V_L \\ I_L \end{bmatrix} = \begin{bmatrix} D & -B \\ -C & A \end{bmatrix} \begin{bmatrix} V_{\text{in}} \\ I_{\text{in}} \end{bmatrix} \tag{6.63}$$

Transmission Lines as Reactive Circuit Elements

In many practical transmission-line applications, transmission-line losses are small and often negligible. In particular, short sections of transmission lines used as circuit elements in high-frequency circuits are often assumed to be lossless.

For a lossless line with $\gamma = j\beta$ and terminated in a complex load impedance Z_L , the input impedance is

$$Z_{in}(\theta) = Z_0 \frac{Z_L + jZ_0 \tan \theta}{Z_0 + jZ_L \tan \theta} \quad (6.64)$$

where $\theta = \beta z' = 2\pi z'/\lambda$ is the electrical distance from the termination. Two particularly important special cases are the short-circuited line with $Z_L = 0$ and the open-circuited line with $Z_L \rightarrow \infty$.

The input impedance of an open-circuited lossless transmission line is

$$Z_{oc} = -jZ_0 \cot \theta = jX_{oc} \quad (6.65)$$

which is purely reactive. The normalized reactance is plotted in Fig. 6.16a. For small line lengths of less than a quarter wavelength ($\theta < 90^\circ$), the input impedance is purely

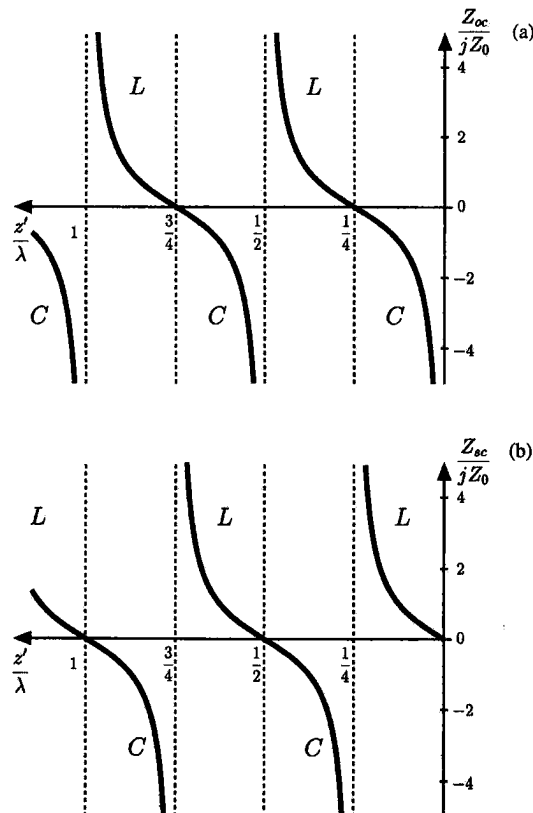


Figure 6.16 Normalized input reactance of a lossless transmission line terminated in (a) an open circuit and (b) a short circuit.

capacitive, as expected. With increasing electrical distance θ , the input reactance alternates every quarter wavelength between being capacitive and inductive. Any reactance value $-\infty < X_{oc} < +\infty$ can be achieved by appropriately adjusting the electrical length (i.e., by varying the physical length or the frequency (wavelength)). Furthermore, for line lengths corresponding to multiples of a half wavelength, the input impedance is again an open circuit. In contrast, for line lengths corresponding to odd multiples of a quarter wavelength, the input impedance is zero [$Z_{oc}(z' = \lambda/4 + n\lambda/2) = 0, n = 0, 1, 2, \dots$].

The input impedance of a short-circuited lossless transmission line is also purely reactive and is given by

$$Z_{sc} = jZ_0 \tan \theta = jX_{sc} \quad (6.66)$$

Figure 6.16b shows the normalized reactance X_{sc}/Z_0 as a function of electrical length θ . For small line lengths of less than a quarter-wavelength ($\theta < 90^\circ$), the input impedance of a short-circuited line is purely inductive, as expected. The dependence of the input reactance of the short-circuited line on electrical length θ corresponds to that of the open-circuited line with a shift by a quarter wavelength. In particular, for line lengths corresponding to multiples of $\lambda/2$, the input impedance is zero, whereas for line lengths corresponding to odd multiples of $\lambda/4$, the input impedance of a short-circuited lossless line is an open circuit [$Z_{sc}(z' = \lambda/4 + n\lambda/2) \rightarrow \infty, n = 0, 1, 2, \dots$].

An important application of open- and short-circuited transmission lines is the realization of reactive circuit elements for example for matching networks and filters, in particular at microwave frequencies ranging from a few gigahertz to tens of gigahertz.* At these frequencies, ordinary lumped elements become exceedingly small and difficult to realize and fabricate. In contrast, open- and short-circuited transmission-line sections with lengths on the order of a quarter wavelength become physically small enough to be realized at microwave frequencies and can be easily integrated in planar circuit technology. In practice, it is usually easier to make a good short-circuit termination than an open-circuit termination because of radiation from the open end and coupling to nearby conductors.

Example. To illustrate the design of reactive transmission-line segments, an equivalent inductance $L_{eq} = 5 \text{ nH}$ and an equivalent capacitance $C_{eq} = 2 \text{ pF}$ are realized

*Open- and short-circuit input impedance measurements for a general lossy transmission line can also be used to determine the transmission-line parameters. From $Z_{oc} = Z_0 \coth \gamma z'$ and $Z_{sc} = Z_0 \tanh \gamma z'$ for a lossy line follows

$$Z_0 = \sqrt{Z_{oc} Z_{sc}} \quad (6.67)$$

and

$$\tanh \gamma z' = \sqrt{\frac{Z_{sc}}{Z_{oc}}} \quad (6.68)$$

However, care should be taken in the extraction of $\gamma = \alpha + j\beta$ from Eq. (6.68) due to the periodicity of the phase term $\beta z'$, which must be approximately known.

at $f = 5$ GHz using a short-circuited $50\text{-}\Omega$ microstrip line with effective dielectric constant $\epsilon_{\text{eff}} = 1.89$. From Eq. (6.66) follows

$$L_{\text{eq,sc}} = \frac{Z_0 \tan \theta_L}{\omega} \quad (6.69)$$

$$C_{\text{eq,sc}} = -\frac{1}{\omega Z_0 \tan \theta_C} \quad (6.70)$$

The minimum electrical lengths for positive values for L_{eq} and C_{eq} are found as $\theta_L = 72.3^\circ$ ($l_L/\lambda = 0.201$) and $\theta_C = 162.3^\circ$ ($l_C/\lambda = 0.451$). With $\lambda = 4.36$ cm the corresponding physical lengths of the short-circuited microstrip segments are $l_L = 0.88$ cm and $l_C = 1.97$ cm.

Complex Reflection Coefficient

The behavior of a terminated line is further examined in terms of incident and reflected waves at the termination. The ratio of the voltage phasors V^- and V^+ at the termination is defined as the voltage reflection coefficient $\Gamma_L = V^-/V^+$ and is given in terms of the load impedance Z_L and characteristic impedance Z_0 as

$$\Gamma_L = |\Gamma_L|e^{j\theta_L} = \frac{Z_L - Z_0}{Z_L + Z_0} \quad (6.71)$$

The load reflection coefficient Γ_L is in general complex. Here, a different symbol than in Eq. (6.23) is used to emphasize the definition of the complex reflection coefficient as ratio of voltage phasors. For a passive load $|\Gamma_L| \leq 1$. If the terminating load impedance equals the characteristic impedance of the line (matched termination), $\Gamma_L = 0$ and $V^- = 0$. For an open-circuit termination, $\Gamma_L = \Gamma_{\text{oc}} = +1$, while for a short-circuit termination, $\Gamma_L = \Gamma_{\text{sc}} = -1$. In general, for a purely reactive termination $Z_L = jX_L$ ($X_L > 0$ or $X_L < 0$) and real characteristic impedance, the magnitude of the reflection coefficient is $|\Gamma_L| = 1$.

Standing Waves

The total voltage and current along a lossless transmission line with $\gamma = j\beta$ can be expressed with reflection coefficient Γ_L at the termination as

$$V(z') = V_0^+ \{e^{+j\beta z'} + \Gamma_L e^{-j\beta z'}\} \quad (6.72)$$

$$I(z') = \frac{V_0^+}{Z_0} \{e^{+j\beta z'} - \Gamma_L e^{-j\beta z'}\} \quad (6.73)$$

The superposition of the two opposing traveling wave components leads to periodic variations in voltage and current along the line due to constructive and destructive wave interference. The resulting wave interference component is known as a *standing wave*. For an arbitrary termination with reflection coefficient $\Gamma_L = |\Gamma_L|e^{j\theta_L}$, the voltage and current

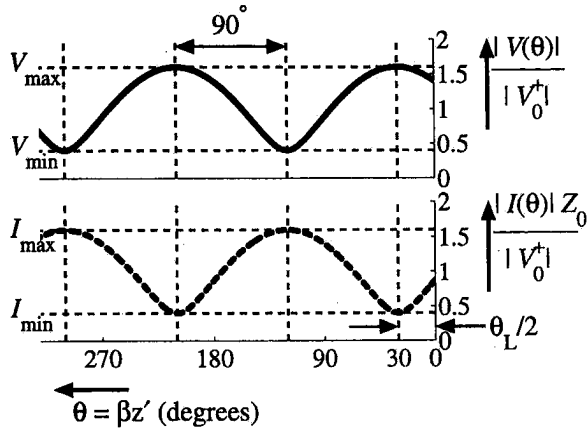


Figure 6.17 Voltage and current standing-wave patterns for a lossless transmission line terminated in a complex load impedance with $\Gamma_L = 0.6 e^{j60^\circ}$.

standing-wave patterns are given by

$$|V(z')| = |V_0^+| \sqrt{(1 + |\Gamma_L|)^2 \cos^2\left(\beta z' - \frac{\theta_L}{2}\right) + (1 - |\Gamma_L|)^2 \sin^2\left(\beta z' - \frac{\theta_L}{2}\right)} \quad (6.74)$$

$$|I(z')| = \frac{|V_0^+|}{Z_0} \sqrt{(1 - |\Gamma_L|)^2 \cos^2\left(\beta z' - \frac{\theta_L}{2}\right) + (1 + |\Gamma_L|)^2 \sin^2\left(\beta z' - \frac{\theta_L}{2}\right)} \quad (6.75)$$

Figure 6.17 illustrates the relative voltage and current variations along a lossless transmission line for a general complex load impedance with $\Gamma_L = 0.6 e^{j60^\circ}$. In general, the standing-wave pattern on a lossless transmission line is periodic with a period of $\lambda/2$ (or 180° in θ). The voltage magnitude alternates between the maximum and minimum values V_{\max} and V_{\min} given by

$$V_{\max} = (1 + |\Gamma_L|) |V_0^+| \quad (6.76)$$

$$V_{\min} = (1 - |\Gamma_L|) |V_0^+| \quad (6.77)$$

Similarly, the maximum and minimum current values I_{\max} and I_{\min} are

$$I_{\max} = (1 + |\Gamma_L|) \frac{|V_0^+|}{Z_0} = \frac{V_{\max}}{Z_0} \quad (6.78)$$

$$I_{\min} = (1 - |\Gamma_L|) \frac{|V_0^+|}{Z_0} = \frac{V_{\min}}{Z_0} \quad (6.79)$$

The locations with maximum voltage can be found from the condition $\beta z' - \theta_L/2 = n\pi$ ($n = 0, 1, 2, \dots$). The minimum voltages are located a quarter wavelength from the maximum voltages. Locations with current maximum correspond to locations with minimum voltage and vice versa.

The ratio of V_{\max} to V_{\min} is defined as the *standing-wave ratio* (SWR, or S for short) and is given in terms of the reflection coefficient at the termination by

$$\text{SWR} = \frac{V_{\max}}{V_{\min}} = \frac{I_{\max}}{I_{\min}} = \frac{1 + |\Gamma_L|}{1 - |\Gamma_L|} \quad (6.80)$$

The standing-wave ratio is a measure for the amount of mismatch at the termination. The standing-wave ratio for a matched termination is $\text{SWR} = 1$. For an open-circuit, a short-circuit, or a purely reactive termination $\text{SWR} \rightarrow \infty$. For a resistive or complex termination, $1 < \text{SWR} < \infty$. In general, SWR varies in the range

$$1 \leq \text{SWR} \leq \infty \quad (6.81)$$

Table 6.3 shows the standing-wave patterns for several special types of terminations. For an open-circuit termination and a purely resistive termination with $R_L > Z_0$, the voltage is maximum at the termination. In contrast, the voltage at the termination is minimum for a short-circuit termination or a purely resistive termination with $R_L < Z_0$. A resistive termination causes a compression in the standing-wave pattern, whereas a reactive termination gives rise to a shift of the voltage maximum away from the termination. For a complex termination as shown in Fig. 6.17 with $\Gamma_L = 0.6e^{j60^\circ}$, the standing-wave pattern is both compressed ($\text{SWR} = 4$) and shifted toward the source side by $\theta_L/2 = +30^\circ$ compared to the open-circuit case.

The standing-wave ratio and the distance from the termination to the nearest voltage maximum can be determined in an experimental setup to find the complex reflection coefficient and, hence, the complex impedance of an unknown termination.* The reflection coefficient magnitude $|\Gamma_L|$ is given in terms of SWR as

$$|\Gamma_L| = \frac{\text{SWR} - 1}{\text{SWR} + 1} \quad (6.82)$$

Example. From standing-wave measurements, the standing-wave ratio is found as $\text{SWR} = V_{\max}/V_{\min} = 5$, the distance between successive voltage minima is 20 cm, and the distance from the termination to the nearest voltage minimum is 4 cm. From Eq. (6.82) follows the magnitude of the reflection coefficient at the termination as $|\Gamma_L| = (5 - 1)/(5 + 1) = 2/3$. The wavelength on the line corresponds to twice the distance between successive voltage minima and is $\lambda = 40$ cm. The distance from the termination to the closest voltage minimum is $4/40\lambda = \lambda/10$ or 36° , and the distance to the nearest voltage maximum is $\lambda/10 + \lambda/4 = 0.35\lambda$ or 126° . The phase of the reflection coefficient is $\theta_L = 2 \times 126^\circ = 252^\circ$. The corresponding load impedance is found with $Z_L = Z_0(1 + \Gamma_L)/(1 - \Gamma_L)$ as $Z_L = (0.299 - j0.683)Z_0$.

In most applications, the phase information for the reflection coefficient is not needed. The magnitude of the reflection coefficient directly determines the fraction of

*In practice, it is easier to accurately determine the location of a voltage minimum. The location to the voltage maximum can be obtained from the location of the voltage minimum by adding or subtracting a quarter wavelength.

Table 6.3 Standing-wave Patterns on a Lossless Transmission Line for Special Types of Terminations

Type of termination	Standing-wave pattern
<p>Open circuit</p> $ V(z') = 2 V_0^+ \cos \beta z' $ $ I(z') = \frac{ V_0^+ }{Z_0} \sin \beta z' $ $\Gamma_L = +1 \quad \text{SWR} = \infty$	
<p>Short circuit</p> $ V(z') = 2 V_0^+ \sin \beta z' $ $ I(z') = 2 \frac{ V_0^+ }{Z_0} \cos \beta z' $ $\Gamma_L = -1 \quad \text{SWR} = \infty$	
<p>Resistive termination $R_L > Z_0$</p> $ V(z') = \frac{2}{R_L + Z_0} V_0^+ \sqrt{R_L^2 \cos^2 \beta z' + Z_0^2 \sin^2 \beta z'}$ $ I(z') = \frac{2}{R_L + Z_0} \frac{ V_0^+ }{Z_0} \sqrt{Z_0^2 \cos^2 \beta z' + R_L^2 \sin^2 \beta z'}$ $\Gamma_L = \frac{R_L - Z_0}{R_L + Z_0} > 0 \quad \text{SWR} = \frac{R_L}{Z_0}$	
<p>Resistive termination $R_L < Z_0$</p> $ V(z') = \frac{2}{R_L + Z_0} V_0^+ \sqrt{Z_0^2 \cos^2 \beta z' + R_L^2 \sin^2 \beta z'}$ $ I(z') = \frac{2}{R_L + Z_0} \frac{ V_0^+ }{Z_0} \sqrt{R_L^2 \cos^2 \beta z' + Z_0^2 \sin^2 \beta z'}$ $\Gamma_L = \frac{R_L - Z_0}{R_L + Z_0} < 0 \quad \text{SWR} = \frac{Z_0}{R_L}$	
<p>Reactive termination $Z_L = jX_L$</p> $ V(z') = 2 V_0^+ \left \cos(\beta z' - \theta_L/2) \right $ $ I(z') = 2 \frac{ V_0^+ }{Z_0} \left \sin(\beta z' - \theta_L/2) \right $ $\Gamma_L = 1e^{j\theta_L}$ $\theta_L = 2 \tan^{-1}(Z_0/X_L) \quad \text{SWR} \rightarrow \infty$	

average incident power that is reflected back on the transmission line. With Eqs. (6.72) and (6.73), the net power flow on a lossless transmission line is given by

$$P_{\text{ave}}(z') = \frac{1}{2} \operatorname{Re}\{V(z')I^*(z')\} = \frac{|V_0^+|^2}{2Z_0} (1 - |\Gamma_L|^2) = P_{\text{ave}}^+ (1 - |\Gamma_L|^2) \quad (6.83)$$

which is independent of position z' on the line. The fraction of average incident power P_{ave}^+ that is reflected is

$$P_{\text{ave}}^- = -|\Gamma_L|^2 P_{\text{ave}}^+ \quad (6.84)$$

The negative sign in Eq. (6.84) indicates the power flow away from the load. Note that the incident power P_{ave}^+ is the combined power due to all forward traveling wave components and thus depends on the load impedance if the source is not matched ($Z_S \neq Z_0$).

In many transmission systems, such as a radio transmitter site, it is critical to monitor the amount of reflected power. The percentage of reflected power can be directly determined from the measured standing-wave ratio. For example, for $\text{SWR} = 1.5$, the magnitude of the reflection coefficient is 0.2, which means that 4% of the incident power is reflected. For a 60-KW transmitter station this would amount to a reflected power of 2400 W.

6.4.3. The Smith Chart

The *Smith chart*, developed by P. H. Smith in 1939, is a powerful graphical tool for solving and visualizing transmission-line problems [17,18]. Originally intended as a graphical transmission-line calculator before the computer age to perform calculations involving complex impedances, the Smith chart has become one of the primary graphical display formats in microwave computer-aided design software and in some commonly used laboratory test equipment, in particular the network analyzer.

The transformation of complex impedance along a transmission line given in Eq. (6.64) is mathematically complicated and lacks visualization and intuition. On the other hand, the reflection coefficient undergoes a simple and intuitive transformation along the transmission line. The reflection coefficient at distance z' from the termination is defined as $\Gamma(z') = V^-(z')/V^+(z')$ and is given in terms of the reflection coefficient at the termination Γ_L by

$$\Gamma(z') = \Gamma_L e^{-j2\beta z'} = |\Gamma_L| e^{j(\theta_L - 2\beta z')} \quad (6.85)$$

The magnitude of the reflection coefficient is unchanged along the lossless line and the phase of the reflection coefficient is reduced by twice the electrical distance from the termination.

The Smith chart combines the simple transformation property of the reflection coefficient along the line with a graphical representation of the mapping of normalized

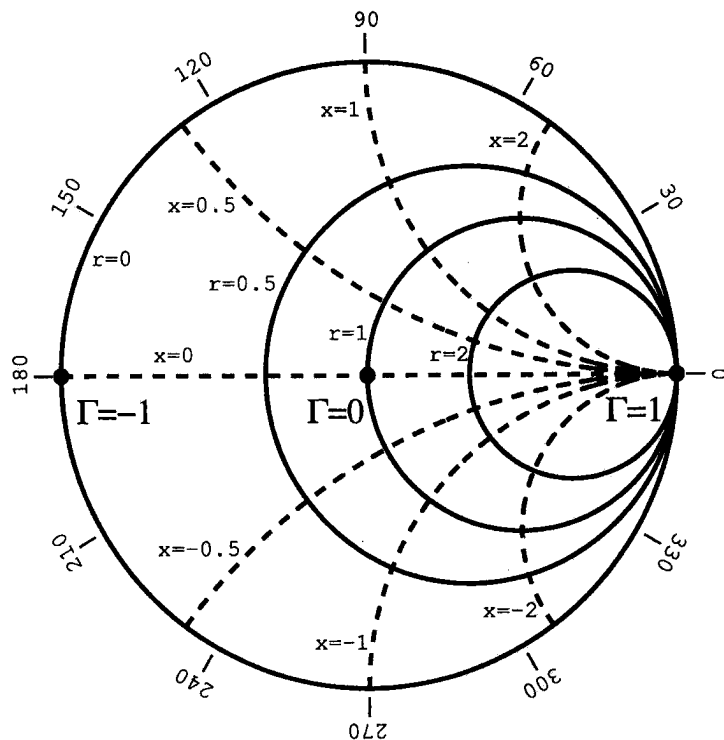


Figure 6.18 Illustration of the basic features of the Smith chart.

impedance to the complex reflection coefficient plane given by

$$z(z') = \frac{Z_{in}(z')}{Z_0} = \frac{1 + \Gamma(z')}{1 - \Gamma(z')} \quad (6.86)$$

Here, $z = r + jx = Z/Z_0$ is defined as the normalized impedance with respect to the characteristic impedance of the line. The combination of these two operations in the Smith chart enables the simple graphical determination and visualization of the impedance transformation along a transmission line. Other parameters, such as the standing-wave ratio or the locations of voltage maxima and minima on the line can be simply read off the Smith chart, and more advanced transmission-line calculations and circuit designs can be performed with the Smith chart.

Figure 6.18 illustrates the basic features of the Smith chart. The chart shows a grid of normalized impedance coordinates plotted in the complex plane of the reflection coefficient. The impedance grid consists of a set of circles for constant values of normalized resistance r and a set of circular arcs for constant values of normalized reactance x . Any normalized impedance $z = r + jx$ on a transmission line corresponds to a particular point on or within the unit circle ($|\Gamma| = 1$ circle) in the complex plane of the reflection coefficient. For a matched impedance the $r = 1$ circle and $x = 0$ line intersect at the origin of the Smith chart ($\Gamma = 0$). The open-circuit point $\Gamma = 1$ is to the far right, and the short-circuit point $\Gamma = -1$ is to the far left, as indicated in Fig. 6.18. In a real Smith chart, as shown

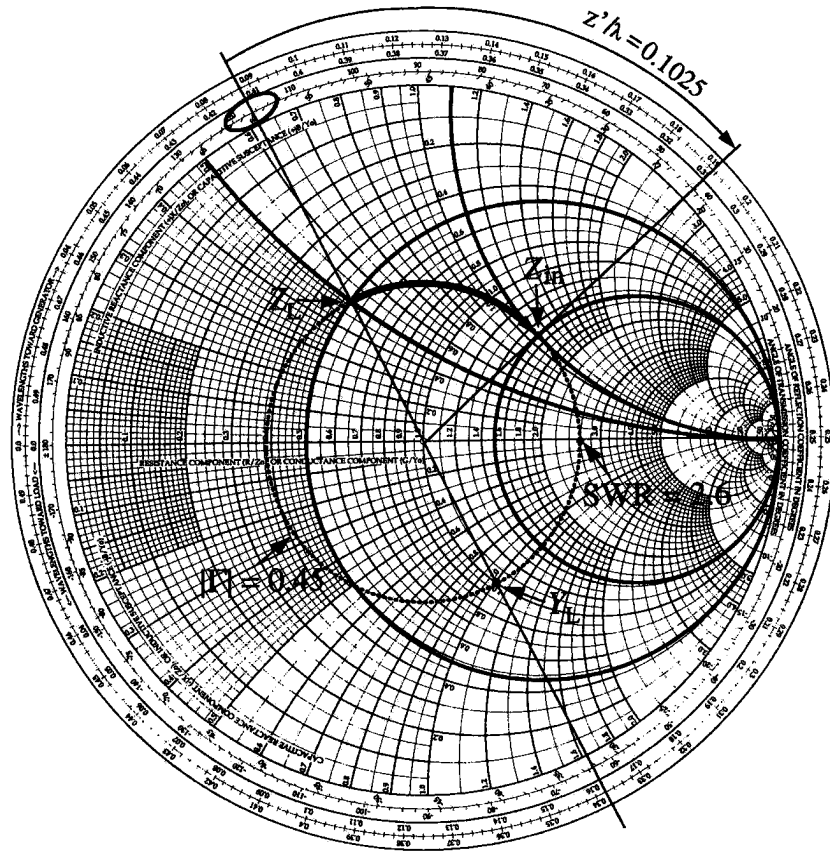


Figure 6.19 Smith chart example for $Z_L = (25 + j25) \Omega$ and $Z_0 = 50 \Omega$.

in Fig. 6.19, a fine grid is used for added accuracy, and scales are added to help with the calculation of phase change in reflection coefficient along the transmission line.

Example. To illustrate the use of the Smith chart for transmission-line calculations, consider a lossless line with characteristic impedance $Z_0 = 50 \Omega$, which is terminated in a complex load impedance $Z_L = (25 + j25) \Omega$. The normalized load impedance is $z = 0.5 + j0.5$ and is shown on the Smith chart as the intersection of the $r = 0.5$ and $x = 0.5$ grid circles. The load reflection coefficient can be directly read off from the Smith chart. The radius of the transformation circle through Z_L (relative to the radius of the unit circle $r = 0$) gives the magnitude of the reflection coefficient as $|\Gamma_L| = 0.45$. The phase of the reflection coefficient is $\theta_L = 116.5^\circ$. The standing-wave ratio on the line corresponds to the normalized maximum impedance z_{\max} along the line, which is real and lies on the intersection of the transformation circle and the $x = 0$ line. The standing-wave ratio can be directly read off the Smith chart as $\text{SWR} = 2.6$. For a given electrical length of the line, the input impedance is found by first determining the reflection coefficient at the input through clockwise rotation on the transformation (SWR) circle by twice the electrical length of the line, as given by Eq. (6.85). Assuming an electrical length of $l = 0.1025 \lambda$, the phase of the reflection coefficient changes by $-2\beta l = -4\pi \times 0.1025$. This amounts to a rotation in *clockwise* direction by about 74° . For convenience, the Smith chart includes scales around its periphery, which can be used to determine the amount of phase rotation directly in

units of wavelengths. In this example, the starting value at the load on the rotation scale labeled "toward generator" is 0.088. The end value is $0.088 + 0.1025 = 0.1905$. The phase of the reflection coefficient is read off as $\theta_{in} = 42.5^\circ$. Finally, the input impedance is obtained as the intersection of the line through the origin with constant phase and the transformation circle. The normalized input impedance is approximately found as $Z_{in} = 1.5 + j1.1$, or $Z_{in}(z' = l = 0.1025\lambda) = (75 + j55) \Omega$.

In transmission-line problems with parallel-connected elements, it is advantageous to work with admittances rather than impedances. The impedance Smith chart can be conveniently used with normalized admittances $y = g + jb = YZ_0$ by considering the relationship

$$\Gamma = \frac{z - 1}{z + 1} = -\frac{y - 1}{y + 1} \quad (6.87)$$

where $y = 1/z$. This relationship shows that the impedance grid can be directly used as admittance grid with $g = \text{const}$ circles and $b = \text{const}$ circular arcs if the reflection coefficient is multiplied by negative one, which amounts to a rotation by 180° on the Smith chart. Then, the open circuit is located at the far left and the short circuit is at the far right. The conversion from normalized impedance coordinates to normalized admittance coordinates given by $y = 1/z$ can be simply achieved on the Smith chart by a 180° rotation along the transformation (SWR) circle. For example, for the normalized load impedance $z = 0.5 + j0.5$, the normalized load admittance is found as $y = 1/z = 1 - j$, as indicated in Fig. 6.19.

6.4.4. Impedance Matching

In many transmission-line applications, it is desirable to match the load impedance to the characteristic impedance of the line and eliminate reflections in order to maximize the power delivered to the load and minimize signal distortion and noise.* Reducing or eliminating reflections from the load is particularly important in high-power RF transmission systems to also minimize hot spots along a transmission line (e.g., the feed line between the transmitter and the antenna) that are caused by standing waves and not exceed the power-handling capabilities of the transmission line. Excessive reflections can also damage the generator, especially in high-power applications.

In practice, the impedance of a given load is often different from the characteristic impedance Z_0 of the transmission line, and an additional impedance transformation network is needed to achieve a matched load condition. Figure 6.20 illustrates the basic idea of matching an arbitrary load impedance Z_L to a transmission line. The matching network is designed to provide an input impedance looking into the network that is equal to Z_0 of the transmission line, and thus eliminate reflections at the junction between the transmission line and the matching network. The matching network is ideally lossless so

In general, impedance matching can be done at the load or the source end, or at both ends of the transmission line. For a matched source, maximum power is delivered to the load when it is matched to the transmission line and power loss on the line is minimized. For a given source impedance Z_S , maximum power transmission on a lossless line is achieved with conjugate matching at the source ($Z_{in} = Z_S^$) [1].

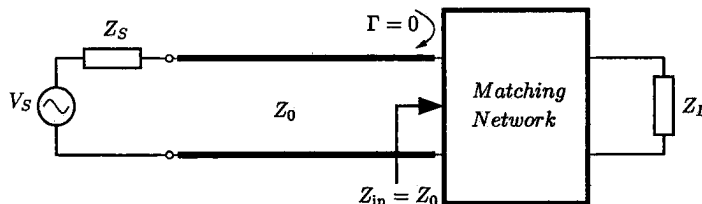


Figure 6.20 General illustration of impedance matching at the termination.

that all incident power on the line ends up being dissipated in the load. A lossless matching network may consist of lumped reactive elements or reactive transmission-line elements (stubs) at higher frequencies and/or cascaded transmission-line sections of appropriate length.

A matching network requires at least two adjustable parameters, such as a lumped series element and a lumped shunt element, each with adjustable reactance value, to independently transform the real and imaginary parts of the load impedance. Because the elements in the matching network are frequency dependent, the exact matching condition is generally achieved only at a single design frequency. For other frequencies, the reflection coefficient will be sufficiently small only over a narrow bandwidth about the design frequency. Larger matching bandwidths may be achieved if more independent elements are used in the matching network.

Many different design choices of matching networks are available. The selection of a particular matching network may depend on a number of factors including realizability in a given technology, required bandwidth, simplicity, occupied space, tunability of the matching network, and cost of implementation. In the following, two common matching methods using sections of lossless transmission lines are described to further illustrate the concept of impedance matching.

Quarter-wave Transformer

A lossless transmission line of length $l = \lambda/4$ has a special simplified impedance transformation property, which can be advantageously used for impedance matching. With Eq. (6.64), the input impedance of a lossless transmission line of length $l = \lambda/4$ and characteristic impedance $Z_{0,T}$ that is terminated with load impedance Z_L is

$$Z_{in}|_{l=\lambda/4} = \frac{Z_{0,T}^2}{Z_L} \quad (6.88)$$

In particular, any purely resistive load impedance $Z_L = R_L$ is transformed into a resistive input impedance given by $R_{in} = Z_{0,T}^2/R_L$. Hence, a quarter-wave section of a transmission line can be directly used to match a purely resistive load impedance R_L to a line with characteristic impedance Z_0 if the characteristic impedance $Z_{0,T}$ of the quarter-wave section is given by

$$Z_{0,T} = \sqrt{R_L Z_0} \quad (6.89)$$

For example, to match a half-wave dipole antenna with input impedance $Z_L \approx 73 \Omega$ to a twin-lead cable with $Z_0 = 300 \Omega$, the characteristic impedance of the quarter-wave transformer should be $Z_{0,T} = \sqrt{73 \Omega \cdot 300 \Omega} \approx 148 \Omega$.

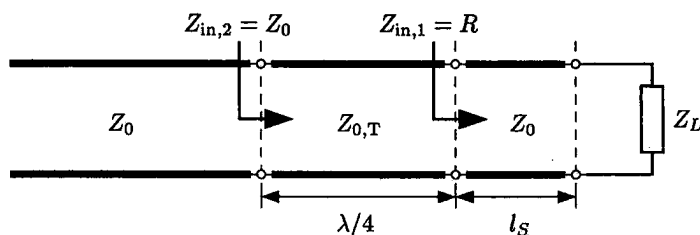


Figure 6.21 Impedance matching of a complex load using a quarter-wave transformer.

If the load impedance is complex, it is necessary to first transform the complex impedance to a real impedance. This can be accomplished with a section of transmission line of appropriate length l_s between the load and the quarter-wave transformer, as illustrated in Fig. 6.21. A transmission line can transform any complex load impedance with $|\Gamma_L| < 1$ to a resistive impedance at the locations with either voltage maximum or voltage minimum. The transmission-line transformation of a complex load to a real impedance is best illustrated on the Smith chart. For example, consider a complex load consisting of a parallel combination of $R_L = 125 \Omega$ and $C_L = 2.54 \text{ pF}$. At the design frequency $f_0 = 1 \text{ GHz}$, the load impedance is $Z_L = (25 - j50) \Omega$. The normalized load impedance $z_L = 0.5 - j$ for $Z_0 = 50 \Omega$ is shown on the Smith chart in Fig. 6.22. The transformation circle intersects the $x = 0$ grid line at $r_{\min} \approx 0.24$ and $r_{\max} = 1/r_{\min} \approx 4.2$. The distance to the closest location with real input impedance ($z_{in} = r_{\min}$) is found as $l_s = 0.135\lambda$. The input impedance at this location is $Z_{in,1} = R = r_{\min}Z_0 \approx 12 \Omega$, and the characteristic impedance of the quarter-wave transformer is found as $Z_{0,T} = \sqrt{RZ_0} \approx 24.5 \Omega$. The second solution with real input impedance is at the voltage maximum with $R = r_{\max}Z_0 \approx 210 \Omega$ and $l_s = 0.135\lambda + 0.25\lambda = 0.385\lambda$. The corresponding characteristic impedance of the quarter-wave transformer is $Z_{0,T} = \sqrt{RZ_0} \approx 102.5 \Omega$. Typically, the solution with the shortest line length l_s is chosen unless it is difficult to realize the characteristic impedance of the corresponding quarter-wave transformer.

Figure 6.23 shows the response of the matching network as a function of frequency. The matching network gives an exact match ($\text{SWR} = 1$) at the design frequency $f_0 = 1 \text{ GHz}$. The bandwidth defined here as the frequency band around the center frequency with $\text{SWR} \leq 1.5$ is about 100 MHz or 10%. The standing-wave ratio response without matching network is also shown in Fig. 6.23 for comparison.

The bandwidth of the matching network can be increased, for example, by cascading multiple quarter-wave sections (multisection quarter-wave transformer) with smaller impedance steps per section giving an overall more gradual impedance transformation [1]. This type of matching network can be easily implemented in planar transmission line technology, such as microstrip, where the characteristic impedance can be changed continuously by varying the line width or spacing.

Stub Matching

In another common impedance matching technique, a reactive element of appropriate value is connected either in series or in parallel to the transmission line at a specific distance from the load. The reactive element can be realized as open- or short-circuited

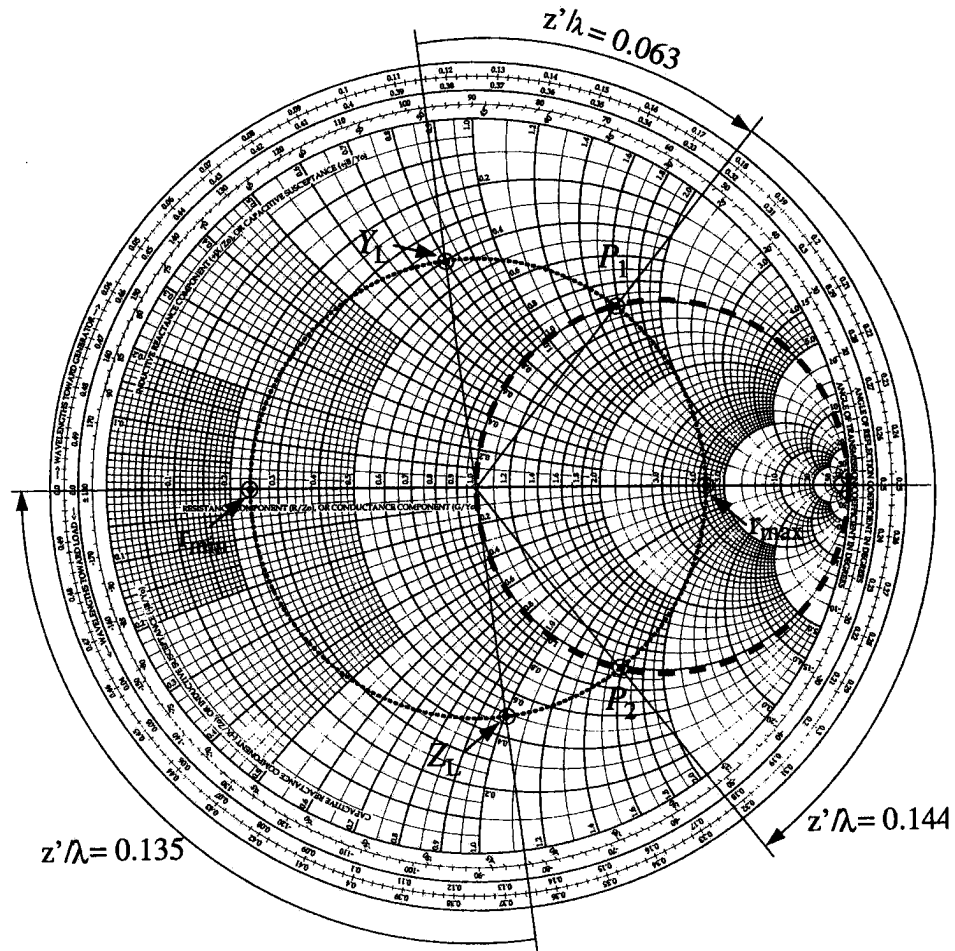


Figure 6.22 Graphical illustration on the Smith chart of quarter-wave matching and shunt (stub) matching of a complex load impedance $Z_L/Z_0 = 0.5 - j$.

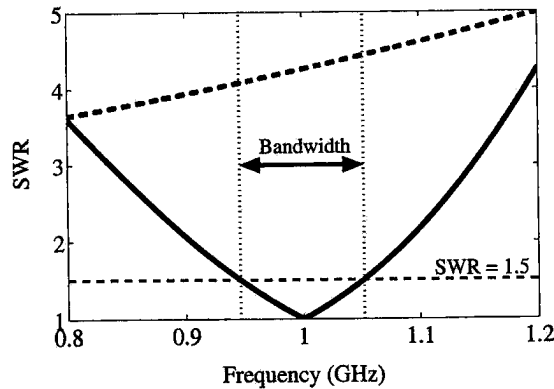


Figure 6.23 SWR=1.5 bandwidth of an example matching network using a quarter-wave transformer. Also shown with a dashed line is the response without the matching network.

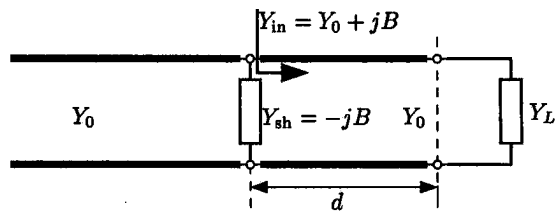


Figure 6.24 Matching network with a parallel shunt element.

stub or as lumped inductor or capacitor element. The two design parameters of a stub matching network are the distance from the termination at which the reactive element is connected, and the stub length needed to realize the required reactance.

The general matching procedure with a single reactive element or a stub is demonstrated for a parallel (shunt) configuration with shunt admittance element Y_{sh} connected at distance d from the termination, as illustrated in Fig. 6.24. For shunt connections it is more convenient to work with admittances than with impedances. The transmission line transforms the load admittance $Y_L = 1/Z_L$ to an input admittance $Y_{in} = G + jB$ at distance d from the termination. In the first step of the matching procedure, distance d is selected such that the real part of the input admittance is matched as $G = Y_0$, and the nonzero input susceptance B is determined. In the second step, a reactive shunt element with admittance $Y_{sh} = -jB$ is added to cancel out susceptance B in the input admittance. The summation of shunt admittance and input admittance of the line yields a matched total admittance $Y_0 = 1/Z_0$.

The shunt matching procedure is further illustrated on the Smith chart shown in Fig. 6.22. The same normalized load impedance $z_L = 0.5 - j$ as in the previous matching network example is assumed. The corresponding normalized load admittance is found from the Smith chart as $y_L = 0.4 + j0.8$. The transformation circle with $|\Gamma| = \text{const}$ intersects the $g = 1$ circle at two points labeled as P_1 and P_2 satisfying the condition $y_{in} = 1 + jb$. Any complex load admittance with $|\Gamma_L| < 1$ can be transformed by a transmission line of appropriate length to a point on the $g = 1$ circle. The normalized input admittances at points P_1 and P_2 are $y_{in,1} = 1 + j1.58$ and $y_{in,2} = 1 - j1.58$, respectively. The distance from the termination to point P_1 on the line with matched real part of the input admittance is found as $d_1 = 0.063\lambda$. The distance to P_2 is $d_2 = d_1 + 0.144\lambda = 0.207\lambda$. The normalized input susceptance $b_1 = 1.58$ at position P_1 is capacitive and needs to be canceled with an inductive shunt element with normalized admittance $y_{sh} = -j1.58$. The required shunt element may be realized with a lumped inductor or an open- or short-circuited stub of appropriate length. Similarly, matching position P_2 with $y_{in,2} = 1 - j1.58$ requires a capacitive shunt element to cancel the susceptance. The capacitive shunt admittance may be realized with a lumped capacitor or an open- or short-circuited stub of appropriate length.

6.5. FURTHER TOPICS OF TECHNOLOGICAL IMPORTANCE AND FUTURE DIRECTIONS

In this section, further transmission-line topics of technological importance are briefly discussed and current developments and future directions are outlined.

6.5.1. Coupled Lines

Transmission-line circuits often consist of multiple parallel conductors that are in close proximity to each other. Examples of multiconductor transmission-line systems include multiphase power lines, telephone cables, and data bus lines on the printed-circuit board (PCB) of a digital system. Due to the proximity of the conductors, the time-varying electromagnetic fields generated by the different transmission lines interact, and the lines become capacitively and inductively coupled. The propagation characteristics of coupled lines depend not only on the line parameters of the individual lines but also on the mutual distributed capacitance and inductance parameters.

The capacitive and inductive coupling between transmission lines often leads to adverse effects in a transmission system. As an example, coupling between closely spaced lines (interconnects) in digital systems can lead to unwanted crosstalk noise and generally sets an upper limit in interconnection density (see e.g. Refs. 10 and 19). On the other hand, electromagnetic coupling between adjacent lines can be used to advantage to realize a variety of components for microwave circuits such as filters, directional couplers, and power dividers [1]. Recently, there has also been increased interest in the realization of compact three-dimensional embedded passive components for RF and mixed-signal modules, and new compact designs using coupled lines have been demonstrated (e.g., Ref. 20). A general overview of coupled transmission-line theory and its application to cross-talk analysis and design of passive microwave components is given, e.g., in Ref. 5.

6.5.2. Differential Lines

A differential line can be considered as a special case of two symmetric coupled lines. A differential line consists of two closely spaced symmetric signal conductors that are driven with identical signals of opposite polarity with respect to a common ground reference (differential signaling). The main advantages of differential lines include an increased immunity to common-mode noise and the localized ground references at the input and output of the line. In particular, the net return current in the ground conductor of a differential transmission line is ideally zero, which helps to eliminate or reduce the effects of nonideal current return paths with finite resistance and inductance. As a disadvantage, differential lines require more conductor traces and generally need to be carefully routed to avoid conversion between differential- and common-mode signals. Because of the advantageous properties of differential lines compared to regular (single-ended) lines, however, differential lines are increasingly being used for critical signal paths in high-speed analog and digital circuits (see, e.g., Refs. 10 and 19). Differential circuit architectures are also being employed in parts of RF circuits because of their superior noise-rejection properties [21].

6.5.3. Chip- and Package-level Interconnects

Transmission lines or electrical interconnects are present at various levels of an electronic system ranging from cabling to printed-circuit board level to chip packaging to chip level. The electrical interconnections in an electronic package constitute the electrical interface between the chip (or a set of chips packaged in a module) and the rest of the electronic system. The package interconnections can generally be represented by a combination of

lumped R , L , C elements and nonuniform coupled transmission lines. In some advanced high-performance packages the interconnections are realized in form of a miniature printed wiring board with several levels of metalization. The electronic package may significantly influence the electrical performance of an integrated circuit; hence, the package characteristics should be included in the design phase of the integrated circuit. The co-design of the integrated circuit and package has recently been pursued for both digital and RF integrated circuits as well as for system-on-a-chip solutions.

At the chip level, interconnects in VLSI and RF integrated circuits usually behave as lumped or distributed RC circuits because of the large series resistance of the metalization. With increasing clock frequencies, however, the distributed series inductance becomes more and more significant. As a result, inductance effects cannot be neglected in some of the longer on-chip interconnects in present-day high-performance VLSI circuits [22]. On-chip interconnects with nonnegligible inductance exhibit transmission-line behavior and need to be modeled as lossy transmission lines rather than RC lines.

6.5.4. CAD Modeling of Transmission Lines

The development of dispersive single and coupled transmission-line models for computer-aided design (CAD) tools is an active area of research in both industry and academia. In general, the line parameters of a transmission line are frequency dependent because of conductor loss (including skin and proximity effects), substrate loss, and dispersion induced by inhomogeneous dielectric substrates. The frequency-dependent transmission-line parameters, however, cannot be represented directly in a time-domain simulator environment such as SPICE. Several approaches for modeling lossy dispersive transmission lines have been developed including (1) convolution with the impulse response of the lossy transmission line, (2) synthesis of the frequency-dependent line parameter in terms of ideal lumped elements and controlled sources for a short line section, and (3) mathematical macromodels obtained with model-order reduction (MOR) techniques resulting in an approximation of the transmission-line characteristics with a finite number of pole-residue pairs. Other areas of current and future interest include the efficient extraction of the line parameters (or parasitics) and the cosimulation of the electromagnetic, thermal, and mechanical phenomena in an electronic system. A review of the methodologies for the electrical modeling of interconnects and electronic packages is given in Ref. 23. Modeling of coupled transmission lines-interconnects based on model-order reduction is further described in Ref. 24.

REFERENCES

1. Pozar, D.M. *Microwave Engineering*, 2nd Ed.; Wiley: New York, 1998.
2. Collin, R.E. *Field Theory of Guided Waves*, 2nd Ed.; IEEE Press: New York, 1991.
3. Cheng, D.K. *Field and Wave Electromagnetics*, 2nd Ed.; Addison-Wesley: Reading, MA, 1990.
4. Ramo, S.; Whinnery, J.R.; Van Duzer, T. *Fields and Waves in Communication Electronics*, 3rd Ed.; Wiley: New York, 1993.
5. Magnusson, P.C.; Alexander, G.C.; Tripathi, V.K.; Weisshaar, A. *Transmission Lines and Wave Propagation*, 4th Ed.; CRC Press: Boca Raton, FL, 2001.
6. Hoffmann, R.K. *Handbook of Microwave Integrated Circuits*; Artech House: Norwood, MA, 1987.
7. Wadell, B.C. *Transmission Line Design Handbook*; Artech House: Norwood, MA, 1991.

8. Nagel, L.W. SPICE: A computer program to simulate semiconductor circuits, Tech. Rep. ERL-M520, Univ. California, Berkeley, May 1975.
9. Johnson, H.W.; Graham, M. *High-Speed Digital Design: A Handbook of Black Magic*; Prentice-Hall: Englewood Cliffs, NJ, 1993.
10. Hall, S.H.; Hall, G.W.; McCall, J.A. *High-Speed Digital System Design: A Handbook of Interconnect Theory and Design Practices*; Wiley: New York, 2000.
11. Freeman, J.C. *Fundamentals of Microwave Transmission Lines*; Wiley: New York, 1996.
12. DeFalco, J.A. Reflection and cross talk in logic circuit interconnections. *IEEE Spectrum* July 1970, 44–50.
13. Oliver, B.M. Time-domain reflectometry. *Hewlett-Packard* Feb. 1964, 15 (6), 1–7.
14. Inan, U.S.; Inan, A.S. *Engineering Electromagnetics*; Addison-Wesley: Reading, MA, 1998.
15. Jong, J.M.; Tripathi, V.K. Equivalent circuit modeling of interconnects from time domain measurements. *IEEE Trans. Comp., Pack., Manufact. Technol.* Feb. 1993, 16 (1), 119–126.
16. Lathi, B.P. *Linear Systems and Signals*; Oxford University Press: New York, 2002.
17. Smith, P.H. Transmission line calculator. *Electronics* Jan. 1939, 12 (1), 29–31.
18. Smith, P.H. An improved transmission-line calculator. *Electronics* Jan. 1944, 17 (1), 130, 318.
19. Dally, W.J.; Poulton, J.W. *Digital Systems Engineering*; Cambridge University Press: New York, 1998.
20. Settaluri, R.K.; Weisshaar, A.; Tripathi, V.K. Design of compact multilevel folded-line bandpass filters. *IEEE Trans. Microwave Theory Tech.* Oct. 2001, 49 (10), 1804–1809.
21. Lee, T.H. *The Design of CMOS Radio-Frequency Integrated Circuits*; Cambridge University Press: New York, 1998.
22. Deutsch, A. When are transmission-line effects important for on-chip interconnections? *IEEE Trans. Microwave Theory Tech.* Oct. 1997, 45 (10), 1836–1846.
23. Ruehli, A.E.; Cangellaris, A.C. Progress in the methodologies for the electrical modeling of interconnects and electronic packages. *Proc. IEEE* May 2001, 89 (5), 740–771.
24. Achar, R.; Nakhla, M. Simulation of high-speed interconnects. *Proc. IEEE* May 2001, 89 (5), 693–728.